122
8-20-75

02-1557

MASTER

UCRL-51802, Pt. 1

EVALUATION OF METHODS FOR SEISMIC ANALYSIS OF NUCLEAR FUEL REPROCESSING PLANTS, PART 1

F. J. Tokarz
R. C. Murray
D. F. Arthur
W. W. Feng
L. H. Wight
M. Zaslawsky

February 7, 1975

Prepared for U.S. Energy Research & Development Administration under contract No. W-7405-Eng-48

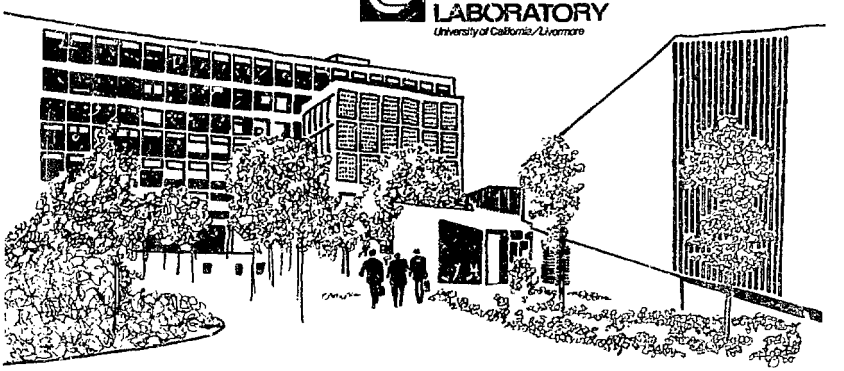

Printed in the United States of America
Available from
National Technical Information Service
U. S. Department of Commerce
5285 Port Royal Road
Springfield, Virginia 22151
Price: Printed Copy $___*; Microfiche $2.25

*Pages	NTIS Selling Price
1-50	$4.00
51-150	$5.45
151-325	$7.60
326-500	$10.60
501-1000	$13.60

Distribution Category
UC-~~80~~ 1C

LAWRENCE LIVERMORE LABORATORY
University of California/Livermore, California/94550

UCRL-51802, Pt. 1

EVALUATION OF METHODS FOR SEISMIC ANALYSIS OF NUCLEAR FUEL REPROCESSING PLANTS, PART 1

F. J. Tokarz
R. C. Murray
D. F. Arthur
W. W. Feng
L. H. Wight
M. Zaslawsky

MS. date: February 7, 1975

Contents

EVALUATION OF METHODS FOR SEISMIC ANALYSIS OF NUCLEAR FUEL REPROCESSING PLANTS, PART 1

Abstract

Currently, no guidelines exist for choosing methods of structural analysis to evaluate the seismic hazard of nuclear fuel reprocessing plants. This study examines available methods and their applicability to fuel reprocessing plant structures. The results of this study should provide a basis for establishing guidelines recommending methods of seismic analysis for evaluating future fuel reprocessing plants.

The approach taken is: (1) to identify critical plant structures and place them in four categories (structures at or near grade; deeply embedded structures; fully buried structures; equipment/vessels/attachments/piping), (2) to select a representative structure in each of the first three categories and perform static and dynamic analysis on each, and (3) to evaluate and recommend method(s) of analysis for structures within each category.

The Barnwell Nuclear Fuel Plant is selected as representative of future commercial reprocessing plants. The Process Building, the Fuel Receiving and Storage Station, and the Waste Tank Cell are selected as representative of near grade, deeply embedded, and fully buried structures, respectively.

The effect of site characteristics on the structural response is also examined. The variation of ground motion with depth for different sites (hard, intermediate, soft) is included.

We recommend the response spectra method of analysis combined with the finite element model for each category. For structures founded near or at grade, the lumped mass model could also be used. If a time history response is required, a time-history analysis is necessary.

Summary and Recommendations

This is the final report of a Lawrence Livermore Laboratory study that was requested and funded by the U. S. Nuclear Regulatory Commission Office of Standards Development. The report is submitted to the Nuclear Regulatory Commission in fulfillment of that request and funding.

Guidelines are needed to specify methods of structural analysis to ensure safe design of critical structures in nuclear fuel reprocessing plants* against

*For some background information on fuel reprocessing facilities see Appendix A.

potential seismic accidents. This study examines available structural analysis methods that can be used to evaluate the earthquake hazard to nuclear fuel reprocessing plants. The results may be used as the basis of a Regulatory Guide that recommends the method of analysis and model necessary to ensure safe design. The study is restricted to fuel reprocessing structures, systems, etc., defined to be critical; i.e., those structures, systems, etc., whose failure could cause a radioactive hazard to the public.

We selected the Barnwell Nuclear Fuel Plant (BNFP)* as representative of future commercial reprocessing plants and took the following approach:

- First, we identified all critical reprocessing plant structures at BNFP.
- Second, to have our results and recommendations represent a large number of structures, we placed these critical structures into four categories which are defined by structural response behavior. These are: (1) structures founded near or at grade, (2) structures deeply embedded, (3) structures fully buried, and (4) equipment/attachments/vessels/piping.
- Third, we selected one representative structure in the first three categories for analysis. The scope of this study did not permit us to address critical structures in the fourth category, such as equipment and piping.
- And fourth, we evaluated the results obtained from each method of analysis. This evaluation includes comparing the results of each method, discussing its shortcomings, and describing the relative computer effort and manpower required.

We believe that this approach is the only practical way to have our analysis results and recommendations represent a large number of structures – that is, by analyzing individual structures in each category, we can generalize the conclusions to all critical structures within that category.

We performed both static and dynamic analyses on each structure selected and include a section discussing the different methods of both site and structural analyses and structural models available to evaluate the earthquake effects on structures.

This study also included a site response analysis to determine the variation of ground motion with depth. We varied site stiffness, thickness, and the level of specified surface acceleration. We concluded that the specified surface acceleration spectrum is an upper bound for the response at depths below the surface for hard and intermediate sites. For soft sites, this is not always true. The analysis and results are included in *Appendix B*.

It should be pointed out that there are many uncertainties associated with the earthquake response of real structures. Much engineering judgement and experience is required to obtain meaningful results. In our analysis, we developed reasonable models to simulate expected structural behavior. We used Regulatory

* BNFP is being constructed in Barnwell County, South Carolina, for Allied-General Nuclear Services and is scheduled to begin operations in 1976 with a nominal fuel reprocessing capacity of 1500 metric tons per year of low-enriched uranium fuels from light-water power reactors.

Guide 1.60 (Ref. 1) to form the basis of input loading, we used state-of-the-art modeling and discretization techniques, and we included the effects of soil-structure interaction in our models. Since it was the purpose of this study to evaluate methods of analysis, no attempt was made to study perturbations in modeling and selection of input parameters which would normally be conducted in analysis for design of real structures. In addition, consideration must be given to the combination of seismic loads with other design conditions (e.g., tornado, wind, dead load, live load, etc.). Current Regulatory guidelines for load combination are summarized in Document A[2] for Category I structures other than containment.

At or Near Grade Structures – For this category, we selected the Process Building (PB) as a representative structure. We compared the results from three different analysis methods for determining earthquake response. The three methods were (1) equivalent static, (2) response spectra, and (3) time-history. A lumped mass model of the Process Building was used for all analyses. All of the results were determined for a 1-g maximum ground acceleration. Displacement, shear, and moment quantities determined by the different methods were compared. The ground motion for all analyses followed the criteria in Guide 1.60. The 5% damped response spectrum was selected.

In addition to comparing the methods of analysis, we studied the effect of site soil properties by examining three sites with different soil characteristics: hard, intermediate, and soft.

We recommend the response spectrum method of analysis with a lumped mass model for structures founded at or near grade. This method produced conservative results with relatively minimal effort.

Fully Buried Structures – For this category, we selected the Waste Tank Cell (WTC) structure as a representative structure. We compared results from three methods for determining earthquake response: (1) the equivalent static, (2) dynamic with a lumped mass model, and (3) dynamic with a finite element model. Both dynamic analyses were conducted using response spectra techniques.

We calculated earthquake loading on the WTC resulting from vertical and horizontal ground motions with each of the three methods and compared the results. We compared displacements, axial and shear forces, and moment quantities. All results were obtained for an earthquake with a maximum ground acceleration of 1 g that follows the criteria established in Regulatory Guide 1.60. The 7% damped response spectrum was used.

We examined the effect of various site conditions (hard, intermediate, and soft) on the calculated loads.

Future WTCs will house a stainless steel tank that contains the radioactive liquid. We therefore considered the effect of the tank and possible sloshing on earthquake design loads.

We recommend the response spectrum method with a finite element model be used to analyze fully buried structures subjected to seismic loading. This method can adequately model the important characteristics of fully buried structures.

Deeply Embedded – For this category we selected the Fuel Receiving and Storage Station as a representative structure. We compared four procedures for calculating seismic loads from horizontal ground motion. Two were equivalent static and two dynamic type of analysis. Both lumped mass and finite element models were used. All analyses were limited to calculating only seismic forces on one embedded wall of the structure.

We believe the walls could be designed statically once the seismic forces have been determined, so we limited our study to comparing various methods of determining seismically induced forces on deeply embedded structures.

All results were obtained for an earthquake with a maximum ground acceleration of 1 g that follows the criteria established in Guide 1.60. The 7% damped response spectrum was used. The effect of the site soil properties were also included in the comparison. Soft, intermediate, and hard sites were considered.

We recommend that the response spectra method with a finite element model be used to determine loads on deeply embedded structures. It alone accounts for all the factors our results show to be important: site response characteristics, soil stiffness, structure stiffness, and soil-structure interface shear forces.

In summary, we recommend that critical structures in fuel reprocessing plants be evaluated against potential seismic hazard using the guidelines shown in Table 1. In addition to the technical comparisons, manpower and computer efforts were considered.

Part 2 of this report will extend the evaluation of methods of structural analysis at reprocessing facilities to equipment and piping (identified in the following section). Other areas within reprocessing facilities which will also be considered in Part 2 include the seismic design of wells, dams, plutonium oxide conversion facilities, and the waste solidification facilities.

Table 1. Recommended models and methods of analysis.

Category	Model	Method of analysis
Structures founded near or at grade	Lumped mass or finite element	Response spectra[a]
Fully buried structures	*Finite element*	*Response spectra*[a]
Deeply embedded structures	Finite element	Response spectra[a]

[a] If a time history of response is required, a time-history analysis must be conducted. If nonlinear effects are considered important (i.e., strain compatible soil properties), a time-history analysis by direct integration must be employed.

Selection of Structures for Analysis

Structures treated in this study should include all types presently anticipated for use in future fuel reprocessing plants. The structures must also reflect structural response characteristics representative of future facilities.

For our analysis, we used the following approach. First, based on USNRC guidance, we selected the Barnwell Nuclear Fuel Plant (BNFP) to be typical of future commercial reprocessing plants. (For further discussion of existing fuel

reprocessing facilities see Appendix A. Included there are discussions on size, type, and location of existing facilities; the reprocessing treatment; treatment of radioactive wastes and gaseous effluents; and plant safety considerations.) We judge both the capacity (1500 metric tons per year) and the process flow, equipment, piping, and structures of BNFP to be representative. Next, we identified all critical structures, equipment, and components within the BNFP facility and placed them into four categories, based on their structural response behavior. Finally, we selected one representative structure from each category for detailed structural analysis and we employed a variety of analysis techniques. With this approach we felt that conclusions drawn from the analysis of each structure could be generalized to all critical structures of that category.

To identify critical structural items, we used the Final Safety Analysis Report[3] for the Barnwell plant as our primary source of information. In addition, we visited Barnwell and the Midwest Fuel Recovery plants, had discussions with USNRC personnel knowledgeable in fuel processing techniques, and met with Bechtel Company personnel who designed the Barnwell facility. These discussions enabled us to develop a better understanding of the structural design basis for the critical structures. This understanding is essential for good structural characterization, which forms the basis for our analyses. We defined critical structures and critical equipment, vessels, and attachments/piping as those whose failure could cause a hazard to the general public.

Table 2 lists the nine major structures that we judged to be critical and places them into categories based on their structural response behavior. These structures are identified in Fig. 1, which shows a plan view of BNFP. Also listed in Table 2 are the critical equipment, vessels, attachments, and piping, and their locations. We excluded the PuO_2 conversion facility and the waste solidification facility from this study, because these structures were still being designed at the time of this investigation. As shown in Table 2, the four categories selected are: (1) structures founded on or near grade, (2) deeply embedded structures, (3) fully buried structures, and (4) equipment vessels/attachments, piping.

The response behavior of deeply embedded structures is generally dominated by soil-structure interaction effects. The response of structures founded near grade is not. For fully buried structures, special attention must be given to vertical response and relative ground displacements. For equipment/vessels/piping, fixed-base models are usually adequate; however, load input definition may be difficult.

We limited this study to the first three structural categories and selected the Process Building (PB), the Fuel Receiving and Storage Station (FRSS), and the Waste Tank Cell (WTC) as representative. We have also conducted a site analysis to provide a reliable definition of input ground motion for structural analysis (see Appendix B). Background information on each of the three structures to be analyzed follows. Figures 2 through 4 give the overall arrangement of the PB and FRSS, and Fig. 5 shows the high-level liquid waste tank (WTC).

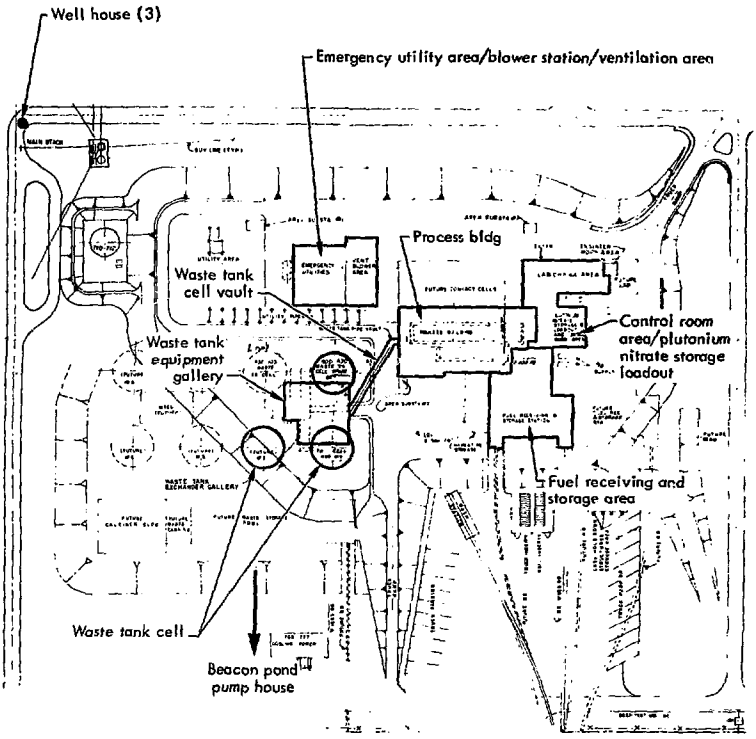

Fig. 1. Plan view of Barnwell Reprocessing Plant.

PROCESS BUILDING

The main process operations at BNFP are housed in a heavily reinforced concrete central structure with walls 3 to 5-1/2 ft thick. The structure is approximately 60 ft wide by 175 ft long by 70 ft high. Figure 2 shows a plan view of a typical plant building, and Figs. 3 and 4 show cross sections of this building.

Within this main central structure are a remote maintenance process cell and a row of contact maintenance process cells. The remote maintenance process cell contains the fuel element shear, the dissolvers, the first cycle solvent

Table 2. Critical[a] structures, equipment, vessels, attachments, piping, etc.

1. Structures Found on or Near Grade

   Process Building (PB)
   Waste Tank Equipment Gallery (WTEG)
   Emergency Utility Area/Blower Station/Ventilation Area (EUA/BS/VA)
   Control Room Area/Plutonium Nitrate Storage Loadout (CRA/PNSL)
   Well House (WH)
   Beacon Pond Pump House (BPPH)

2. Deeply Embedded Structures

   Fuel Receiving and Storage Station (FRSS)

3. Fully Buried Structures

   Waste Tank Cells (WTC)
   Waste Tank Pipe Vaults (WTPV)

4. Equipment/Vessels/Attachments/Piping

   PB

   High activity waste reboiler
   High activity waste concentrator
   Supports (fuel transfer table, conveyor, diverter)
   Shield hatch and windows
   Off gas heater
   Pulse Columns
   Surge tanks (1SF & 1BP)
   HAP heater
   Plutonium product storage, rework and sample tanks
   Plutonium product pump
   Exhaust ducts

   FRSS

   Fuel storage cannisters and brackets
   Emergency water lines
   Cask barrier beams
   Crane rail retainers

   WTEG

   Intermediate-level liquid waste diverter
   High-level liquid waste diverter

   EUA/BS/VFS

   Blowers, doors, filters

   BPPH

   Diesel oil tank and emergency cooling water pumps

   PB/PNSL

   Control room console
   Valve, sample, load-out, maintenance, and pump glove boxes
   Glove box filter frames
   Tank vault cooling units
   Plutonium nitrate storage tanks
   Plutonium nitrate transfer pump

[a]Seismic Category I (for definition see Appendix A).

extraction vessels, and evaporators for highly radioactive solutions.

Remotely operated manipulators and maintenance cranes permit routine process operations and equipment removal, repair, and replacement without entry into the cell. These operations are viewed and controlled from work areas in the galleries above and beside the cell, shielded with 5-1/2 ft of concrete or the equivalent in shielding glass windows. Facilities are provided for repair of the manipulators

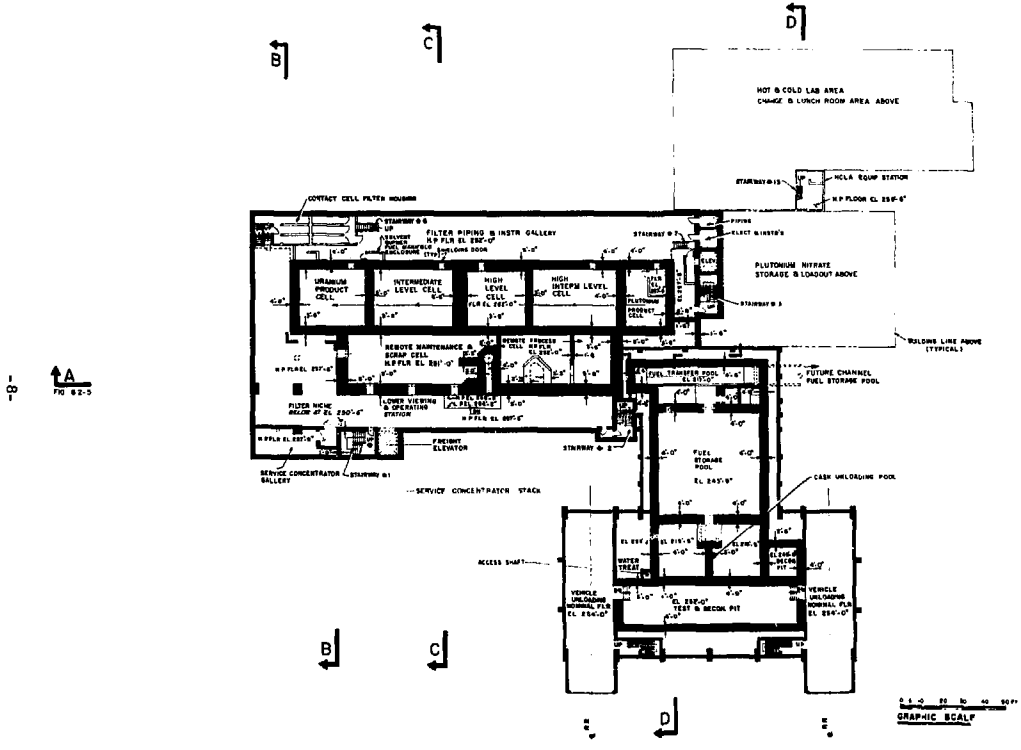

Fig. 2. Plan view of general arrangement of Barnwell Process Building and Fuel Receiving and Storage Station.

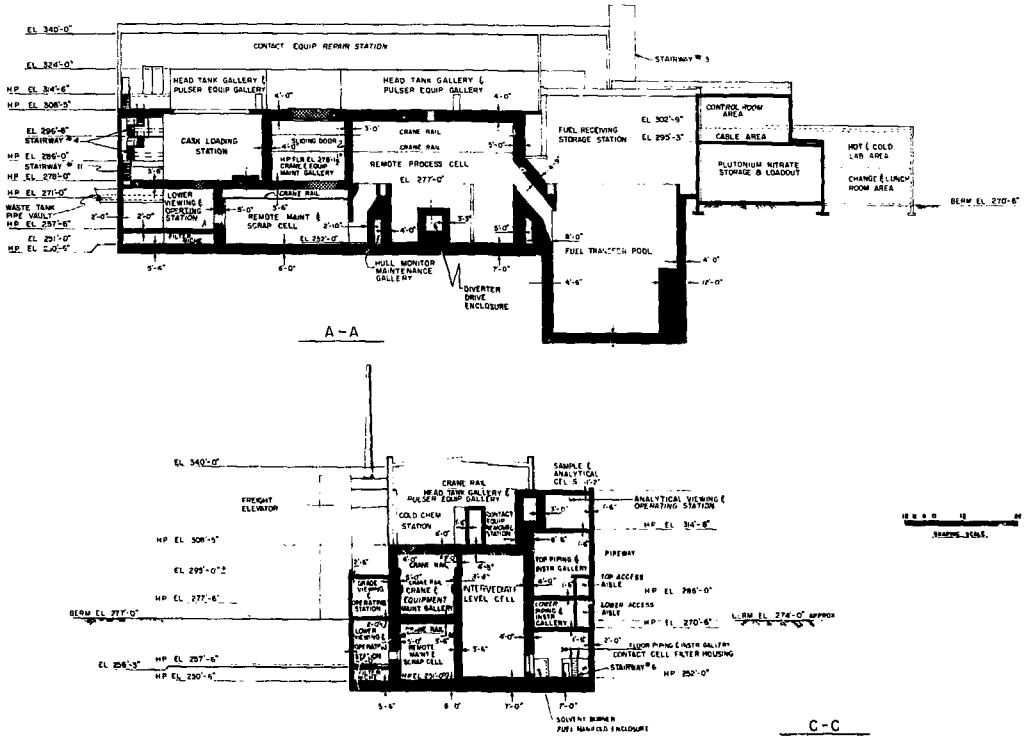

Fig. 3. Cross sections of general arrangement of Barnwell Process Building and Fuel Receiving and Storage Station.

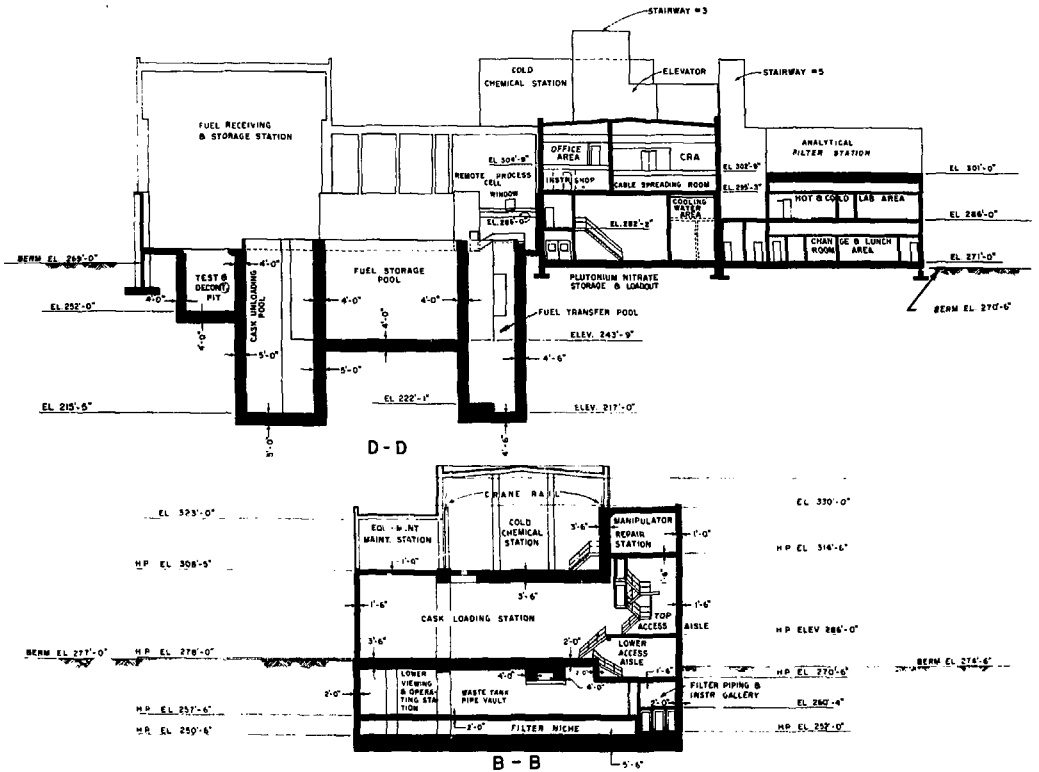

Fig. 4. Cross sections of general arrangement of Barnwell Process Building and Fuel Receiving and Storage Station.

and cranes, for cleanup of contaminated equipment that is to be removed for repair, and for packaging and removal of radioactive solid wastes.

The remote maintenance cell and the contact maintenance cells have stainless steel floor pans to contain spilled fluids. All process cells are divided by shielding walls.

FUEL RECEIVING AND STORAGE STATION

The fuel receiving and storage facility will be used for unloading fuel from shipping casks and short-term storage of the fuel prior to reprocessing. Casks will be transferred by a 150-ton crane to a 55-ft-deep pit in the pool. While under water, the fuel elements will be removed from the casks and transferred to fuel storage canisters by an unloading crane. The loaded canisters will then be transferred to the 28-ft-deep pool storage area. Portions of the pool walls and bottom are lined with stainless steel for additional integrity.

WASTE TANK CELL

Most high-level liquid waste from commercial fuel reprocessing operations will be stored as a concentrated, slightly acidic solution in cooled, corrosion-resistant, 14,000-gal stainless steel tanks. These tanks will be contained in a stainless-steel lined, reinforced concrete vault buried under 10 ft of earth for shielding.

All piping, tanks structures, and cooling systems associated with the waste storage system are designed with a high degree of containment to ensure isolation of radioactive materials from the environment. Process piping to and from the waste tanks is encased. Ventilation air from the vessels is routed to appropriate vessel off gas and ventilation treatment systems in the main process building.

Each high-level waste tank has multiple sets of cooling coils to remove the design maximum heat load from the stored waste. Cooling water circulates through a closed loop system from the tank coils to a heat exchanger and circulation pump. The heat exchanger is cooled with well water and the uncontaminated cooling water discharges to the cooling tower and then to the creek.

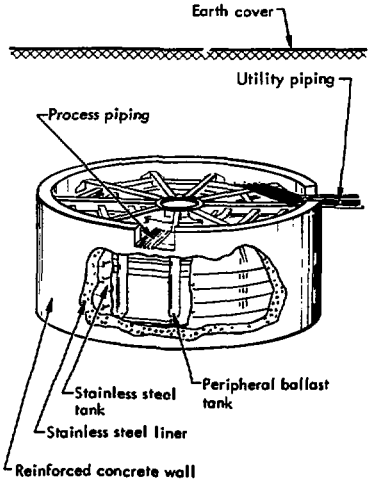

Fig. 5. High-level liquid waste tank.

Selection of Ground Motion and Damping

We needed seismic input for both the site analysis and the structural analysis. Because there are no existing guidelines for the selection of the seismic input to fuel reprocessing plant structures, we had two alternatives: (1) to select a single recorded earthquake accelerogram, or (2) to derive an accelerogram that statistically represents a typical accelerogram. We have chosen the latter approach. Rather than perform the statistical calculations ourselves, we have, for convenience, used the information in USNRC Regulatory Guide 1.60 (Ref. 1).

Guide 1.60 defines the seismic input to nuclear power reactors based on a statistical treatment of some 50 earthquake records. It gives both horizontal and vertical response spectra for different values of structural damping. Both are normalized to a maximum horizontal ground acceleration of 1.0 g. Once the intensity of ground motion for a site is specified in terms of maximum horizontal ground acceleration, both horizontal and vertical spectra can be defined simply by scaling.

The spectra given in Guide 1.60 are based on values one standard deviation over calculated mean spectral accelerations. Guide 1.60 is intended for sites underlain by either rock or soil deposits and it covers all frequencies of interest. For unusually soft sites, modification of this procedure is required. Guide 1.60 is applicable to any epicentral range to the causative earthquake.

We have used the Guide 1.60 statistics to define our input response spectrum. The response spectrum is sufficient seismic input for many structural response calculations (e.g., those calculations based on the response spectra). However, we require a time-history accelerogram as input to our site analysis calculations and to our time-history structural response calculations.

We generated accelerograms compatible with the response spectra with the code SIMEAR.[4] For site seismic analysis input, we used the mean value spectral accelerations[5] at 5% damping, as shown in Fig. 6. Note that these accelerations are one standard deviation below the Guide 1.60 accelerations. We constructed a synthetic accelerogram with SIMEAR, subject to the following constraints: (1) total duration of 30 sec, (2) duration of strong shaking of 8 sec, and (3) onset of strong shaking after 9 sec. We present

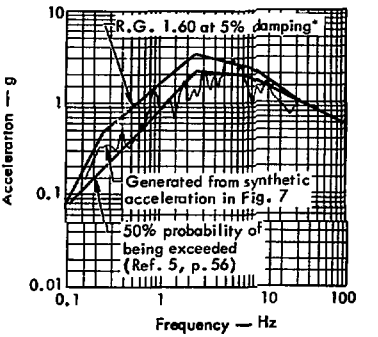

Fig. 6. Ground motion response spectra used for site response analysis. *One standard deviation over average (15.8% probability of being exceeded).

the accelerogram in Fig. 7 and we compare its response spectrum with the mean value response spectrum in Fig. 6. Only horizontal site response analysis was considered.

The ground motion input to a structural analysis should generally be the result of a site analysis. However for this study, we chose the seismic input independent of the site analysis. This was done (1) because the site analysis was conducted at the same time as the structural analysis, and (2) for consistency of seismic input to each structure. We selected the Guide 1.60 5% spectrum as input for the Process Building and the Guide 1.60 7% spectrum as input for the Waste Tank Cell (WTC) and the Fuel Receiving and Storage Station (FRSS). These spectra are shown in Fig. 8. We used the higher damping for the latter structures to account for a greater soil-structure interaction. We

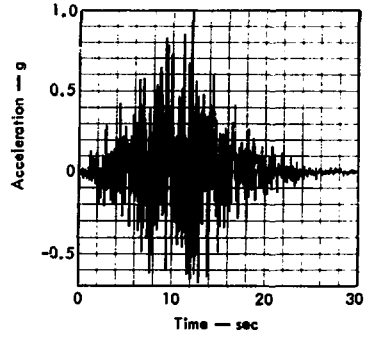

Fig. 7. Ground motion accelerogram used for site response analysis.

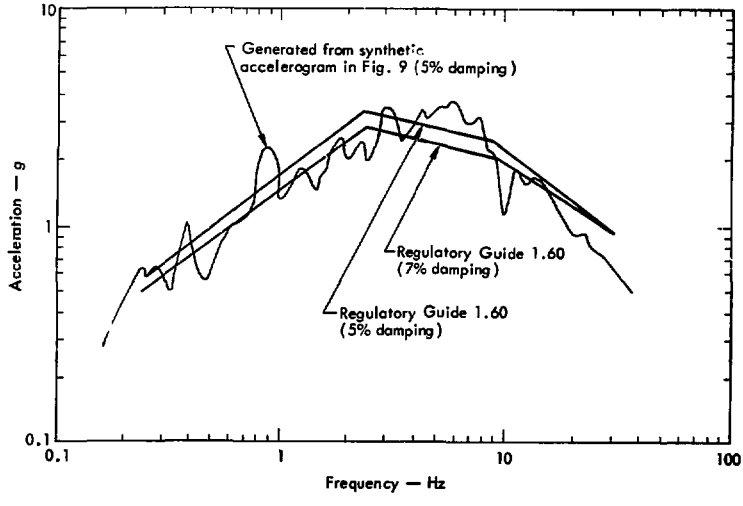

Fig. 8. Ground motion response spectra used for structural analysis.

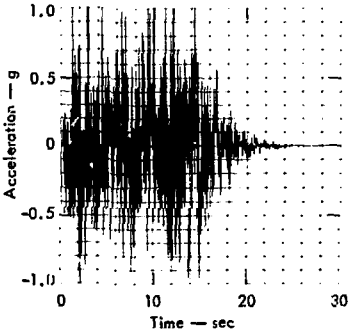

Fig. 9. Ground motion accelerogram used for structural analysis.

developed an equivalent synthetic accelerogram subject to the following parameters: (1) total duration of 30 sec, (2) 10 to 15 sec of strong shaking, and (3) onset of strong shaking at 2 sec. Figure 9 shows this accelerogram. In Fig. 8, we also compare the response spectra at 5% damping. For vertical response calculations, we used the horizontal spectral values.

Damping values used are consistent with Regulatory Guide 1.61 (Ref. 1), which delineates damping values acceptable for elastic dynamic analysis. The damping values account for energy dissipation and reflect both material and structural damping for stresses less than yield.

Methods of Analysis

Seismic analyses of structural systems require (1) definition of the seismic input, generally through a site analysis, (2) construction of a mathematical model of the structure, and (3) selection and application of a method of analysis to calculate the structural response. We discuss below the methods available for each of these steps.

SITE ANALYSIS*

The purpose of a site analysis is to *define the seismic input to structures* founded at the site. Because structures may be founded at or near grade, deeply embedded, or buried, the seismic input may be required either at the surface (in the first case) or below the surface at the foundation level (in the other two cases).

There are three parts to any site analysis: (1) characterizing the earthquake source, (2) characterizing the effect of the seismic travel path from source to the base of the site, and (3) characterizing the effect of the travel path through the site. The analysis for items 1 and 2 is largely empirical and is well covered in the literature. We shall restrict ourselves to methods of analysis *of item 3, the site response. We limit* our discussion to computer methods because of the complexity of the calculation.

The greatest analytical difficulty is the nonlinear behavior of soils, but other complexities include:

(1) Site stratigraphy. The soil layers at the site may not be horizontal and may even be inclined with respect to each other.

*We are providing a section on site analysis methods for completeness. This does not necessarily mean we endorse these methods for reprocessing licensing.

(2) The effect of the water table and soil moisture on the response. For example, the presence of water may discontinuously change the soil equation of state.

(3) The geometry of the seismic input. The emerging seismic energy may be inclined to the soil layers.

Although we can model all of these complexities, some simplifying assumptions are often made and their consequences examined on a case-by-case basis. Assumptions common to the site analysis computer codes most frequently used are:

(1) The response of the site is dominated by horizontal shaking from below. All other modes of seismic energy are neglected.

(2) The horizontal shaking is unidirectional and the site responds with a state of plane strain.

(3) The stress-strain trajectories within the site are cyclic.

(4) There is no residual displacement.

(5) There is no liquefaction of soils.

Each of the codes we use deals with the nonlinear soil properties through the method of equivalent linear systems. In this method the analyst supplies starting values of the shear moduli and damping factors and the code iterates, changing the shear moduli and damping factors to values compatible with the strains experienced during the prior iteration. Shear modulus and damping factor relations have been developed by Seed and Idriss[6] for sands, clays, and rocks, and we describe their specific application in a later section.

It should be noted that there are many uncertainties in modeling a site and the selection of input parameters for analysis. This type of analysis generally requires much experience and judgment on the part of the analyst.

We use three computer codes for site analyses.* These codes represent the state-of-the-art for calculating site response:

PLUMP – Lumped mass[7]
SHAKE – Wave propagation[8]
LUSH – Finite element.[9]

PLUMP – PLUMP calculates the one-dimensional horizontal response of the site. It represents the soil deposit by a series of horizontal layers as shown in Fig. 10. The mass of each layer is lumped at the top and bottom of the layer and the masses are connected by shear springs whose characteristics are specified by the shear stress-shear strain properties of the soil in the layer. The site model is then excited with an acceleration-time history applied at the base of the site. The program will compute horizontal displacements, accelerations, stresses, and strains throughout the site as functions of time.

SHAKE – This code, like PLUMP, calculates the one-dimensional response of horizontal soil layers to horizontal shear shaking. The method of solution is based on the Fourier transformation of the wave equation and the input accelerogram; thus the calculation resembles a systems response calculation (see Fig. 11).

*The use of certain specific analytical techniques and computer codes does not necessarily imply endorsement for use in reprocessing licensing.

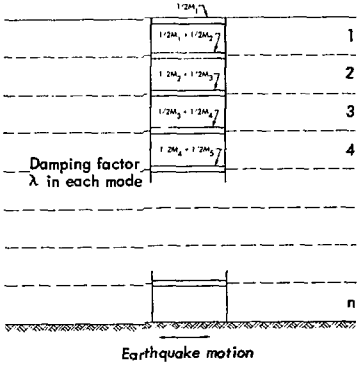

Fig. 10. Lumped mass representation of layered system – PLUMP.

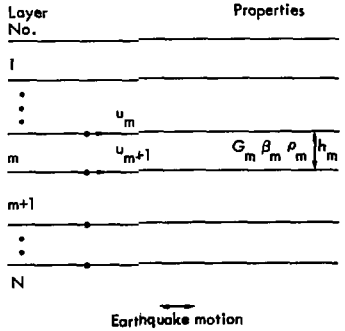

$G_m, \beta_m, \rho_m, h_m, u_m$ = shear modulus, damping factor, mass density, thickness, and response of layer m, respectively.

Fig. 11. One-dimensional representation of layered system – SHAKE.

Because all calculations are in the frequency domain, the code can calculate the response anywhere in the deposit, given the input motion anywhere else in the deposit. Displacement, acceleration, and soil stress, time-histories at any level can be computed with SHAKE.

LUSH – LUSH is a two-dimensional finite element code which solves the transient response problem in soil sites by complex frequency response. It can calculate the response of sloping soil layers to shear shaking emerging at any angle of incidence (see Fig. 12). There are a variety of boundary conditions available and the coding provides for three different materials: nonlinear clays and sands, elastic solids, and rigid solids. LUSH was written specifically to treat site response problems and therefore has incorporated some of the most recent thinking regarding soil deposit response. For example, the material damping can vary from element to element through the method of complex response with complex moduli. Second, because of this approach, accurate solutions can be obtained even in the high frequency range. This is often a requirement for calculations of soil-structure interaction of critical structures.

STRUCTURAL MODEL

Once the seismic input to a structure has been defined, a mathematical model of the structure must be constructed. The model must incorporate all the important response characteristics of the actual structural system being analyzed (e.g., mass and stiffness distributions, structural damping, and

pertinent effects of soil-structure interaction). The mathematical model constructed is usually too complex to solve directly so approximation solution schemes are employed. Either of two methods can be employed to discretize the structure: the lumped mass approach or the finite element approach.

The lumped mass approach divides the structural system into discrete mass points connected by massless springs that represent the stiffness characteristics of the structure. These springs may represent truss members, beam members, or shear panels. An example of a simple lumped mass model is shown in Fig. 13. In this example, the real structure is a process building. In the lumped mass model, the actual mass is concentrated at the appropriate level in the model and the stiffness of the structure is modeled with beam elements that reflect both the bending and shear stiffness of the real structure.

The finite element approach is a technique for discretizing a structure into an assemblage of structural elements. Each element models the mass and stiffness distribution of part of the structure. The mathematical model constructed may be composed of different types of elements to represent differences in structural behavior. Elements are currently available to model truss, beam, continua, plate, shell, and pipe behavior. The use of the finite element procedure eliminates the need to approximate continuous structures by lumped mass systems. Figure 14 shows a finite element representation of a process building. This model uses truss, beam, continua, and plate elements to model the structure.

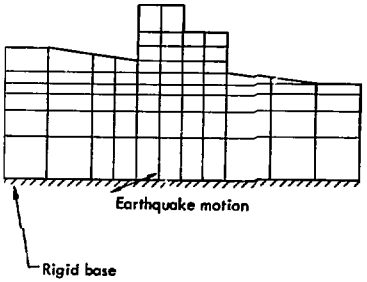

Fig. 12. Typical finite element model—LUSH.

Soil-structure interaction effects must sometimes be included in the mathematical model. Soil-structure interaction is the phenomenon in which the structural response deforms the surrounding soil and consequently modifies the soil motion. This results in a structural response that is generally different from the response that would be calculated using unmodified free-field soil motion. The interaction can often be neglected for very soft structures because of their compliance with the

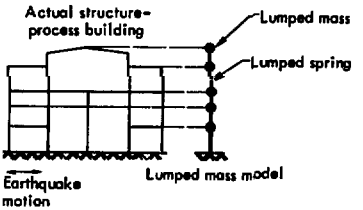

Fig. 13. Lumped mass representation of structural system.

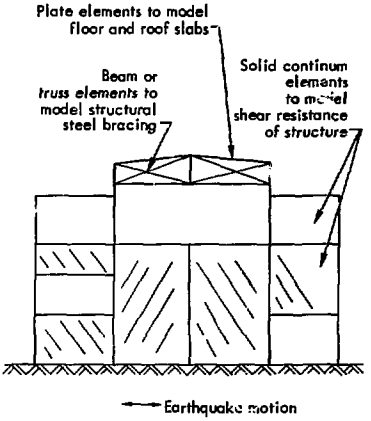

Fig. 14. Finite element representation of a structural system. Figure 13 shows the actual structure-process building.

soil motion. However, it is important to include interaction effects for the stiffer structures that are typical in fuel reprocessing plants.

There are two calculational methods available to represent the effect of the soil:

- applying the soil motion to springs that are attached to the foundation, called the half-space method
- placing the foundation in or on a finite element mesh, and calculating the response of the entire assembly.

Figure 15 is an example of a lumped mass and finite element representation of a process building that includes the effects of soil-structure interaction.[10]

There are limitations to each method. A number of these are summarized in Table 3. The principal advantage of the half-space approach is its simplicity and economy. For example, in Table 4 and Fig. 16 we give formulas for calculating the spring constants.[11] These values were developed for rigid circular and rectangular foundations resting upon the surface of an elastic half space.

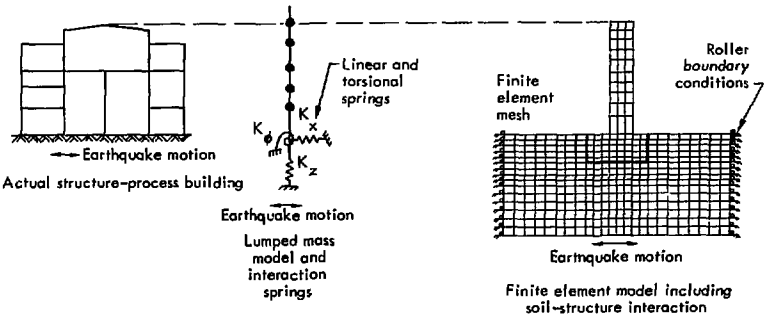

Fig. 15. Lumped mass and finite element representation[10] of soil-structure interaction effects.

Table 3. Limitations of the half-space and finite element methods.

Limitations of half-space method	Limitations of finite element method
• Does not include material and radiation[a] damping.	• Appropriate three-dimensional codes are not available. Presently requires a plane strain solution.
• Cannot model a multilayer soil deposit easily.	• High-frequency information may be lost because of mesh size or the use of Rayleigh damping.
• Neglects structure - structure interaction.	• The extent of the model may not be sufficient to eliminate wave reflections from boundaries.
• No rational way to deal with embedded structures.	• Analysis is more complex than half-space method.
• Does not permit detailed structural analysis.	

[a]Radiation damping accounts for the energy lost by radiation of waves from the base of the structure.

Table 4. Formulas for calculating soil-spring constants[a] for a lumped mass model as shown in Fig. 15.

Motion	Circular foundation	Rectangular foundation
Vertical	$K_z = \frac{4Gr_o}{1-\nu}$	$K_z = \frac{G}{1-\nu}\beta_z\sqrt{BL}$
Horizontal	$K_x = \frac{32(1-\nu)Gr_o}{7-8\nu}$	$K_x = 2(1+\nu)G\beta_x\sqrt{BL}$
Rocking	$K_\phi = \frac{8Gr_o^3}{3(1-\nu)}$	$K_\phi = \frac{G}{1-\nu}\beta_\phi BL^2$

where:

G = Shear modulus of soil (lb/ft^2)

ν = Poisson's ratio of soil (dimensionless)

r_o = Radius of foundation (ft)

B = Foundation dimension perpendicular to applied force (ft)

L = Foundation dimension parallel to applied force (ft)

$\beta_x, \beta_z, \beta_\phi$ = Functions of L/B and are shown in Fig. 16 (dimensionless).

[a]These equations only apply to structures founded at grade. They do not adequately represent deeply embedded or buried structures.

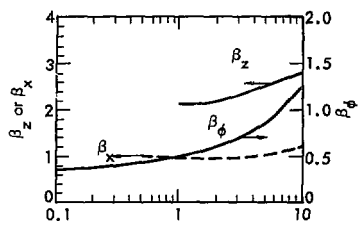

Fig. 16. Soil-structure interaction coefficients for rectangular footing.[11]

STRUCTURAL ANALYSIS

Once the mathematical model has been developed, a method of analysis must be chosen. The purpose of the analysis is to estimate maximum stresses and displacements and to use these estimates to develop a safely designed structure. The methods of structural analysis can be divided into two main categories: equivalent-static and dynamic. The static methods of analysis attempt to furnish a distribution of seismic forces that approximate distributions obtained from dynamic analyses. The dynamic analyses include the inertia effects of the structure as well as the time-varying nature of the forces in the analysis.

Probabilistic methods are also available to conduct seismic analysis. However further research in this area is required before these methods will be useful; they are therefore not considered in this study.

We will consider the following methods of analysis shown in Fig. 17.

Equivalent-Static Methods

These methods of analysis are used to obtain a set of static lateral (horizontal) forces for structural design. The lateral

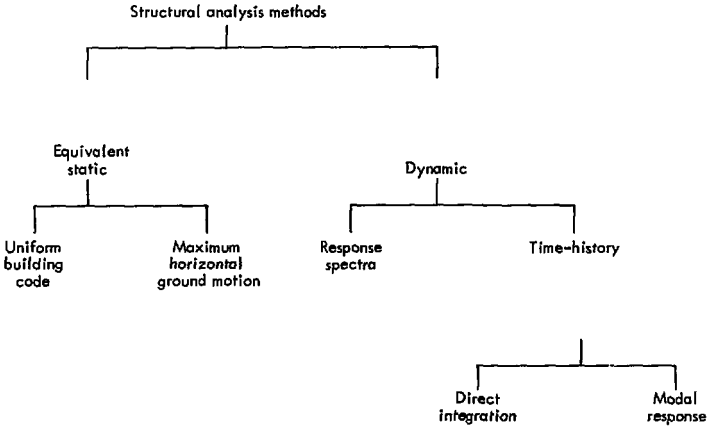

Fig. 17. Structural analysis methods.

forces are generally assumed proportional to the weight of the structure as

$$F = C'W ,$$

where

- F = total effective equivalent static lateral force
- W = weight of structure (includes dead weight plus percentage of live load assumed to be effective during earthquake).
- C' = seismic coefficient.

The selection of the seismic coefficient depends on the seismicity and soil characteristics at the site as well as the dynamic characteristics, type, and function of the structure. The major difference between the different static methods is the way in which the seismic coefficient, C', is obtained. There are two commonly used ways to obtain a value for C': the Uniform Building Code[11] approach and the maximum horizontal ground motion approach. Both of these static methods of analysis assume the structural behavior is governed by the response of the first fundamental mode of vibration.

(1) Uniform Building Code Approach[12]

The method of seismic analysis specified in the Uniform Building Code is a static method of analysis intended for the design of most residential, industrial, and commercial structures in the United States.

This approach provides minimum standards to make structures earthquake-resistant by

- resisting minor earthquakes without damage
- resisting moderate earthquakes without structural damage
- resisting major earthquakes without collapse (could produce severe structural damage).

Many municipalities adopt the Uniform Building Code for minimum design requirements.

In the Uniform Building Code approach, the entire effect of seismic forces on the structure is expressed in terms of base shear. For design, the base shear is distributed as concentrated forces located at various heights. The Uniform Building Code specifies a seismic coefficient that is a function of the natural period of the structure, the seismicity of the area, and the type of structural system employed in the design. The equation for base shear is

$$F = C'W = ZKC\,W,$$

where

- F = base shear
- Z = seismicity factor
- K = type of structure factor
- C = coefficient which is a function of fundamental period of the structure.
- W = total weight of structure

These factors reflect both the seismicity of the area and the actual performance of multistory structures in the United States during earthquakes.

The Building Code also specifies the method of distributing the seismic forces at various levels of the structure, as follows:

$$F_i = F \frac{W_i X_i}{\sum W_i X_i},$$

where

F_i = design force at location i, where i specifies a level of the structure

W_i = weight at location i

X_i = height to location i.

Currently the Uniform Building Code does not use a site factor to include the effect of the type of soil at the site or an importance factor for the structure.

It is not reasonable to use the Uniform Building Code approach directly for the design of critical structures in nuclear facilities. These structures are different from those on which the Building Code is based. Moreover, critical nuclear facilities are required to function during and after a strong earthquake with little or no structural damage.

(2) Maximum Horizontal Ground Motion Approach

Another approach to equivalent static analysis is to use the maximum horizontal acceleration postulated for the site as the seismic coefficient, C'. This would better incorporate the local seismicity of the area into the design but would not include the dynamic characteristics of the structure. In many cases, this is an acceptable approach for stiff structures (i.e., structures with frequencies greater than 33 Hz). A set of static forces for design could be obtained by the Building Code method of distribution.

An example of the equivalent-static method of analysis applied to the Process Building is shown in Fig. 18.

Dynamic Methods

Dynamic methods of analysis determine the distribution of forces in a structure by including the dynamic characteristics of the structure (mass, damping, and stiffness) in the equations of motion. The following methods are generally employed:

(1) Spectra Response Method

This is an approximate method of analysis that requires an acceleration response spectrum as a description of the ground motion. Mode shapes and frequencies of the mathematical model must be calculated. The solution is then obtained by calculating the response (i.e., displacement, acceleration, and

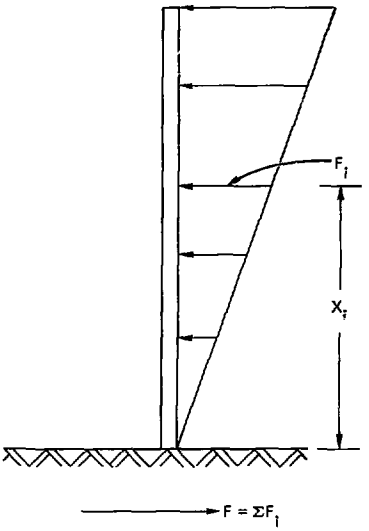

Fig. 18. Example of equivalent static method applied to process building.

stress) in each mode and then adding up the modal responses to get the total response. Figure 19 shows the process.

This mode superposition is usually achieved by a square root of the sum of the squares (SRSS) procedure.* This method of analysis is approximate because of the way the modal quantities are combined to get the total response. The SRSS procedure of combining modal quantities is used since the maximum value in each mode may not occur at the same time. Enough modes must be included in the analysis to capture the complete structural response.

The advantages of this approach over static methods are: (1) the mass and the stiffness characteristics of the structure can be included in the analysis, and (2) the method permits the incorporation of the site response characteristics.

(2) Time-History Method

The time-history method of analysis is an exact method for determining the structural response to an arbitrary force-time history or acceleration-time history. The method solves the following system of equations at each time-step:

$$\underline{M}\,\ddot{\underline{X}} + \underline{C}\,\dot{\underline{X}} + \underline{K}\,\underline{X} = \underline{F}(t),$$

where

$\underline{M}$ = mass matrix

$\underline{C}$ = damping matrix

$\underline{K}$ = stiffness matrix

$\underline{X}, \dot{\underline{X}}, \ddot{\underline{X}}$ = displacement, velocity, and acceleration vectors. (These vectors will have as many entries as degrees of freedom allowed in the model.)

$\underline{F}(t)$ = input forcing function or base acceleration.

Time history analysis is conducted by one of two approaches: mode superposition or direct integration. The mode superposition approach first solves the eigenvalue problem associated with the model to determine the mode shapes and frequencies of vibration. Then the total response is separated into the response of each mode, and finally the response in each mode is determined and combined to get the total response. This method is limited to the linear response of structures.

The direct integration method is used to obtain a solution by step-by-step integration of the equations of motion directly. Solution of the eigenvalue problem is not required and nonlinear effects may be included if required. The method gives an exact time history of response, and a technique to combine modal response is not needed.

A direct integration analysis is equivalent to an analysis by the mode

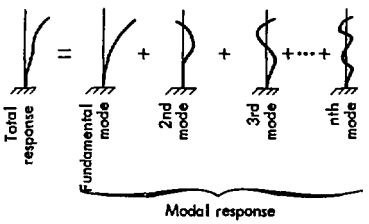

Fig. 19. Schematic of modal superpostion.

*This procedure is modified when closely spaced modes occur in a problem. (Refer to R.G. 1.92.[13]) Another procedure is to combine modal results by adding absolute values of each mode.

superposition approach in which all mode shapes and frequencies are included and the same time step, Δt is used. Both methods involve a large amount of computer time to solve for the dynamic response of a structure, since small time steps are required to achieve meaningful results.

Table 5 compares some of the advantages of these methods.

Computer Programs Used in Structural Analysis*

The structural analysis can be performed by many available computer programs. We conducted our analysis with the SAPIV[14] and GHOSH[15] programs. SAPIV is a structural analysis program for computing the static and dynamic response of three-dimensional linear systems. The structural system that can be analyzed may be modeled with a combination of different structural elements. The program contains the following elements: 3-dimensional truss element, 3-D beam element, plane stress element, plane strain element, 2-D axisymmetric solid element, 3-D solid element, thick shell element, thin plate or shell element, pipe element, and boundary element. These structural elements are shown in Fig. 20. They may be used to model problems for static or dynamic analyses.

GHOSH is a structural analysis program for computing the static and dynamic response of axisymmetric structures (structures that are bodies of revolution) subjected to arbitrary loading or base acceleration. The structural system to be analyzed may be constructed with axisymmetric solid and shell elements.

Both programs can solve static problems and have three solution options for dynamic problems: response spectra analysis, time-history analysis by mode superposition, and time-history analysis by direct integration.

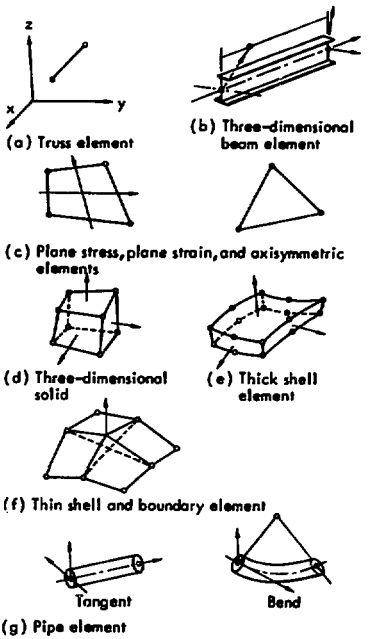

Fig. 20. Element library of SAP IV.

*The use of certain specific analytical techniques and computer codes does not necessarily imply endorsement for use in reprocessing licensing. They are used only to evaluate acceptability of structural design methods.

Table 5. Advantages and disadvantages of methods of analysis.

	Method	Advantages	Disadvantages
Equivalent static	Static	1. Structure usually statically determinate which greatly simplifies structural analysis.	1. No guarantee that equivalent static forces represent actual dynamic loading. 2. Cannot obtain time-history of response.
Response spectra	Response spectra approach	1. Faster than both time-history methods for most problems with base acceleration. 2. Provides a simple way of determining maximum response quantities. Results reasonably accurate. 3. Spectra bounding many earthquake acceleration-time history may be used as input.	1. Solution of large eigenvalue problems can be time consuming. 2. Must combine maximum modal quantities to get total solution. 3. Cannot obtain time-history of response. 4. Limited to base acceleration inputs only.
Time-history	Direct integration of equations of motion	1. Can include non-linear material and geometric effects. 2. For very large problems may be faster than mode superposition methods. 3. Time-history of response obtained directly. 4. Approximations involved in neglecting higher modes in mode superposition method not needed. 5. Results accurate for a given acceleration-time history.	1. Usually requires a large amount of computer time to solve problem. 2. Results from different acceleration-time histories both consistent with the same response spectra may be different.
	Integration of uncoupled modal equations	1. Faster than direct integration for most problems, since solution may be expressed by first few modes. 2. Once frequencies and mode shapes are obtained a variety of response analysis can be conducted efficiently. 3. Results accurate for a given acceleration-time history. 4. Time-history of response obtained directly.	1. Solution of large eigenvalue problems can be time consuming. 2. Not applicable to non-linear analysis. 3. Results from different acceleration-time histories both consistent with the same response spectra may be different.

Process Building (PB)

INTRODUCTION

We compare the calculated results obtained by using three different analysis procedures for determining the seismic response of near-grade or partially embedded structures. We use the Process Building (PB) as representative of this category of structure. The three methods of analysis conducted on the Process Building were:

- Equivalent static method
- Response spectra method
- Time-history methods

The same lumped mass model of the Process Building was used for all analyses.

All results were determined for a 1-g maximum ground acceleration. Since all materials were linear-elastic, the response to other peak accelerations can be obtained by linear scaling. The ground motion for all analyses was horizontal and met the criteria established in Guide 1.60 (Ref. 1). The 5% damped response spectrum was used. The damping value of 5% is appropriate for the concrete structure but may be low for soil behavior. For the purposes of this comparison, 5% damping was assumed for both concrete and soil.

We also studied the effect of site soil properties by examining three sites with different soil characteristics: hard, intermediate, and soft. The effects of the site soil conditions were included in the analysis by translational and rotational soil springs developed for elastic half spaces. Alternative ways to develop equivalent soil springs exist but were not included in this evaluation.

MODEL DESCRIPTION

The Process Building is typical of structures founded near grade or partially embedded. Figure 21 shows plan and elevation views of a representative process building. This structure is the same as the one at the BNFP facility. Future designs may provide a corridor between the five process cells and the remote process cell. This will cause the building to be slightly wider but should have little effect on the seismic analysis.

The Process Building is a heavily reinforced, massive, concrete structure with many cells for confinement of chemical reprocessing equipment. We used a lumped mass model to represent the dynamic response of the building, as shown in Fig. 22. This model represents the properties of the Process Building in the transverse direction. The methods of analysis and comparison discussed here apply equally well to the longitudinal direction.

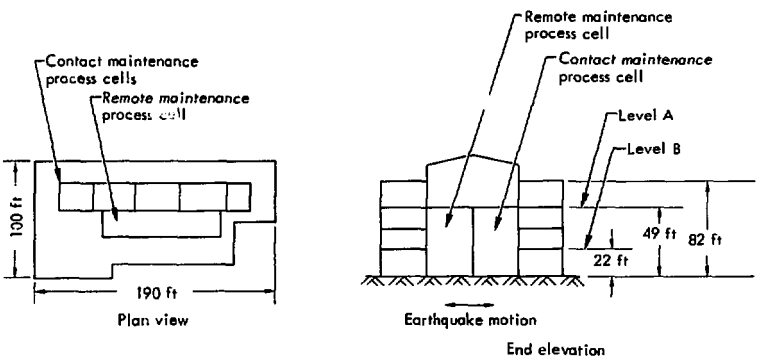

Fig. 21. Plan and elevation views of a typical process building.

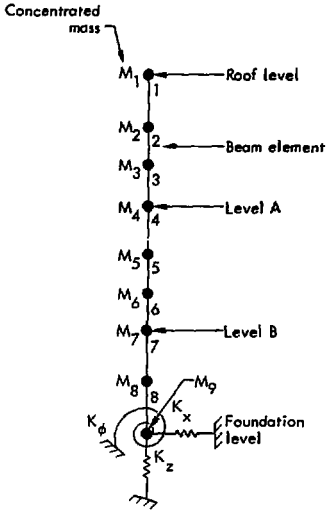

Fig. 22. Lumped mass model of process building.

Masses were lumped at regions where heavy floors or other concentrated weights occur. Beam elements were used to represent the shear stiffness of the reinforced concrete shear walls. Reinforced concrete floor slabs act as rigid horizontal diaphragms and cause the building to move laterally as a unit.

Soil-springs were included in the model at the base of the structure to consider soil-structure interaction effects. The spring constants were varied to study the effects of different site properties on the structural response. The properties reflected hard, intermediate, and soft sites and were defined by their shear wave velocities. Table 6 lists the material properties used in this analysis.

Properties of the shear beams were computed from cross-sectional geometry data at various elevations in the Process Building.[3] These values represent characteristics of the BNFP Process Building. Values used for the lumped masses and the beam properties are given in Table 7. Shear stiffnesses were determined from $A_s G/L$, where A_s is the effective resisting shear area, G is shear modulus of concrete, and L is the length of shear beam. Values for the spring constants, K_x, K_z, K_ϕ, were determined using Table 4 and are shown in Table 8. We assumed a rectangular foundation with

Table 6. Process Building material properties.[a]

	γ (lb/ft^3)	C_s[b] (ft/sec)	ν	E (10^6 lb/ft^2)	G (10^6 lb/ft^2)
4000-psi concrete	150.0	–	0.25	550.0	220.0
Soft soil	125.0	500.0	0.30	2.5	1.0
Intermediate soil	125.0	2000.0	0.30	40.4	15.5
Hard soil	125.0	4000.0	0.30	162.0	62.2

[a]Damping is assumed to be a uniform 5% of critical damping for the entire soil-structure system.

[b]Shear wave velocity $C_s = \sqrt{G/\rho}$, ρ = mass density = γ/g.

Table 7. Properties of Process Building used for analysis.

Location	Mass (kip-sec^2/ft)	Shear stiffness (10^6 kip/ft)	Height above grade (ft)
1	70	1.5	82
2	100	5.5	66
3	240	26.8	58
4	150	42.1	49
5	230	21.1	42
6	230	62.3	28
7	240	26.7	22
8	260	46.8	8
9	650	–	0

dimensions 100 by 190 ft for this analysis.

More detailed and complex structural models can be constructed. We believe these models would not give us any more information about the overall structural behavior of the Process Building.

METHODS OF ANALYSIS

Equivalent-Static Method

We chose one static method of analysis. It is based on F = C'W, where F is the equivalent static load from the earthquake to be applied to the structure, C' is the seismic coefficient, and W is the weight of the structure. We used a value of C' = 1 g, which assumes that the seismic coefficient C is equal to the peak horizontal ground acceleration and that no dynamic amplification of the structure would occur. The earthquake loads were distributed as discussed in the methods of analysis section.

Results of the static analysis are shown in Fig. 23. These figures show the variation of lateral displacement, shear, and moment with height for the Process Building.

Response Spectra Method

The response spectra method is an approximate-solution technique for determining maximum displacements, shears, and moments from earthquake excitation. In this approach the input base motion is a response spectrum.

We did three response spectra analyses on an intermediate site that differed in the number of modes of vibration included in the solution. We used one, five, and nine modes. One mode is the minimum number required to obtain a solution and nine modes is the maximum number we can use for the mathematical model of the Process Building.

Our calculations show that the structural response is governed by the first mode and that the response is unaffected if additional modes are included. Accordingly, we use only the first mode solution for the three sites considered (see Fig. 24.)

Table 8. Spring constants.

Site characteristic	k_x (10^6 kip/ft)	k_z (10^6 kip/ft)	k_ϕ (10^{10} kip-ft/rad)
Soft site	0.36	0.45	0.13
Intermediate site	5.7	7.2	2.1
Hard site	22.8	28.8	8.2

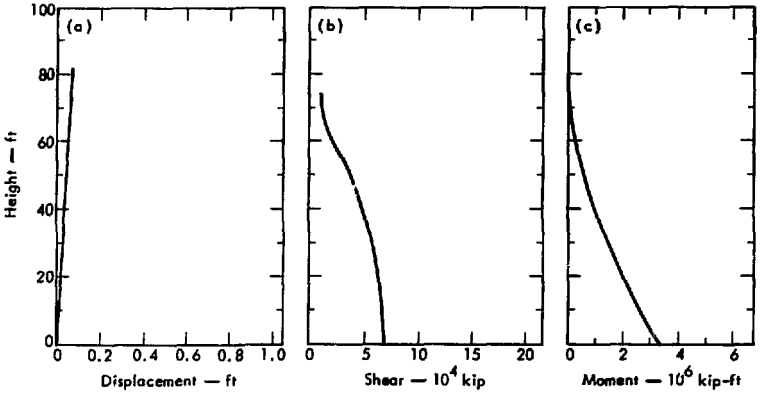

Fig. 23. Static results for the Process Building. (a) Variation of lateral displacement with height. (b) Variation of shear with height. (c) Variation of moment with height.

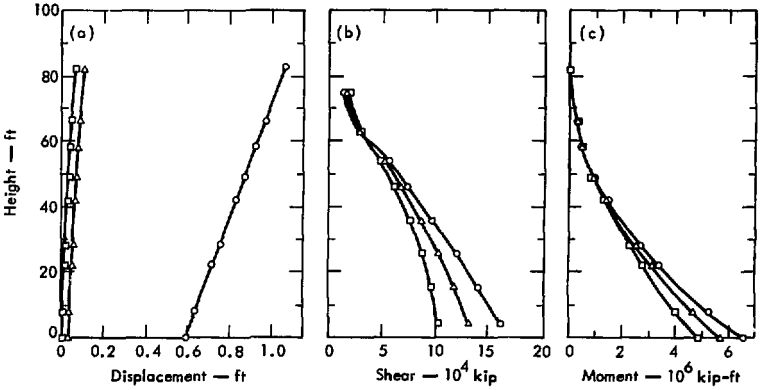

Fig. 24. Response spectra results for the Process Building. (a) Variation of lateral displacement with height. (b) Variation of shear with height. (c) Variation of moment with height. Symbols: o — soft soil; Δ — intermediate soil, and □ — hard soil.

Time-History Methods

Time-history methods of analysis are exact methods for determining the response of a structure of time-varying forcing functions or to base acceleration time-histories. There are two approaches available for conducting a time-history analysis: mode superposition and direct integration.

First we compared the mode superposition and direct integration approaches, using the model shown in Fig. 22. In both cases the acceleration time-history defined in Fig. 9 was applied at the foundation level.

Table 9 gives the results of these analyses. They differ very little. Because the response of the structure was

Table 9. Comparison of results of time-history analyses for an intermediate site.

Location	Displacement (ft)		Shear (10^4 kip)		Moment (10^6 kip-ft)	
	Direct integration	Mode superposition	Direct integration	Mode superposition	Direct integration	Mode superposition
1	0.242	0.246	0.98	1.09	0.0	0.0
2	0.212	0.215	0.98	1.09	0.16	0.17
3	0.198	0.200	2.25	2.45	0.34	0.37
4	0.185	0.186	4.78	5.12	0.77	0.83
5	0.175	0.175	6.23	6.67	1.21	1.30
6	0.154	0.154	8.35	8.80	2.38	2.53
7	0.145	0.145	10.17	10.58	2.99	3.17
8	0.126	0.125	11.86	12.21	4.59	4.81
9	0.115	0.113	13.42	13.61	5.69	5.93

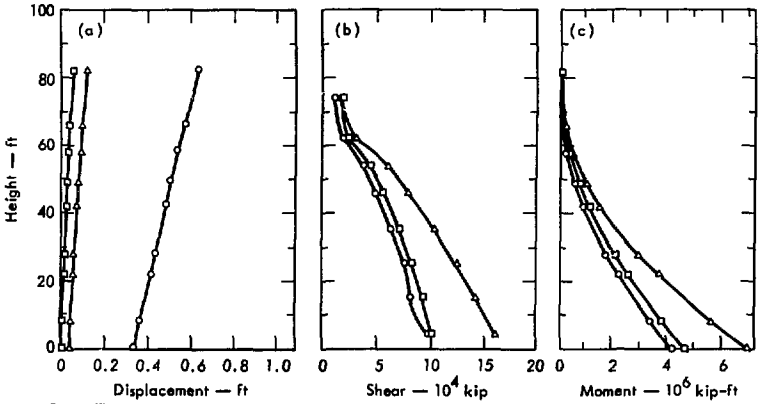

Fig. 25. Time-history results for the Process Building. (a) Variation of lateral displacement with height. (b) Variation of shear with height. (c) Variation of moment with height. Symbols: ○ — soft soil; △ — intermediate soil, and □ — hard soil.

governed by the first mode of vibration, the mode superposition method is more economical than the direct integration method.

Results of time-history analyses for all three sites are shown in Fig. 25. These analyses were all conducted with an input acceleration time-history applied at the base level.

Effect of Site Characteristics on Analysis

Time-history and response spectra analyses were conducted on the Process Building model located on sites of different stiffness. The effect of site stiffness was included in the model as translational and rotational springs. Values for these spring constants were determined from the equations presented in the section on methods of analysis. Site characteristics were defined by shear wave velocity through the soil.

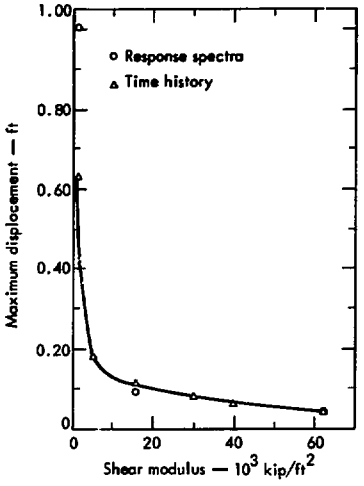

Fig. 26. Effect of site characteristics on maximum displacement.

Table 10 and Figs. 26 through 28 show maximum results from these analyses. These results indicate little difference between methods for hard sites and a large difference for soft sites. For the intermediate site, we found differences in the methods. Since the structural response of the Process Building is governed by the first mode response, we believe that these differences result partly from differences between the Guide 1.60 spectra and the spectrum of the acceleration time-history used in analysis. As the site becomes very soft (i.e., as the shear modulus approaches zero), the results obtained from a time-history analysis tend to their limiting values. (Displacement goes to maximum ground displacement, base shear goes to zero, and moment at base goes to zero.) Caution should be used in comparing these methods for very soft sites.

Table 10. Summary of maximum displacements, shear, and moment calculated by different methods for the three sites considered.

Site	Displacement (ft)		Base shear (10^4 kip)		Overturning moment (10^6 kip-ft)	
	Response spectra	Time history	Response spectra	Time-history	Response spectra	Time history
Soft	1.05	0.60	16.2	9.2	6.6	3.8
Intermediate	0.10	0.12	13.1	16.0	5.7	7.0
Hard	0.06	0.05	10.2	10.1	4.9	4.7

We compared these spectra for 5% damping. The differences for the sites studied are shown in Fig. 29. Both methods give equivalent results for hard sites, but they are sensitive to the generated acceleration time-history and the integration time step for softer sites. The time-history method can produce results higher or lower than those obtained by the response spectra method, depending on the position of the generated spectra with respect to the Guide 1.60 spectra. This difference alone is not enough to explain the difference in results.

Care must therefore be taken in generating an artificial acceleration time-history. This generated accelerogram should produce a spectrum which minimizes the differences in the methods. The time step for integrating should also be small enough to capture the complete response.

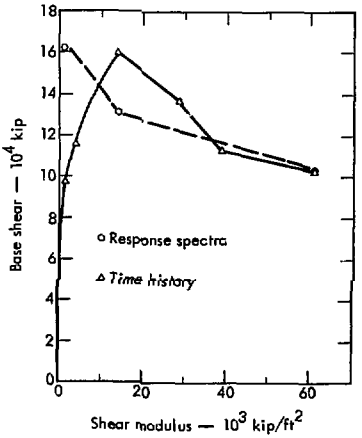

Fig. 27. Effect of site characteristics on base shear.

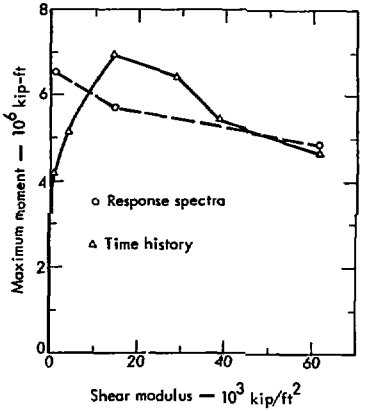

Fig. 28. Effect of site characteristics on overturning moment.

For the soft site there was essentially no difference between the spectra, but the difference between methods was the largest. We believe this difference results from the way soil-structure interaction was included in the model and the time step of integration chosen. The soft spring could be acting as a filter for time-history analysis.

COMPARISON OF METHODS

Results of our analyses are compared in Figs. 30 through 32. These analyses used the same mathematical model and an earthquake with a peak horizontal ground acceleration of 1 g. The 1-g maximum ground acceleration was used directly to conduct the static analysis. The horizontal spectrum for 5% damping in Guide 1.60 was used directly as input for the response spectra analysis, and

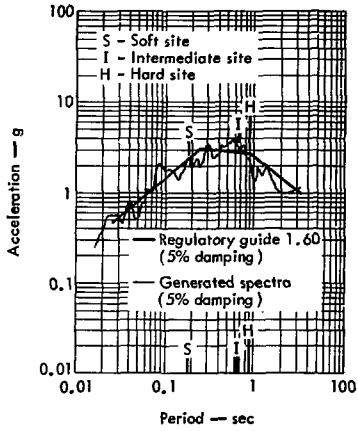

Fig. 29. Comparison of regulatory guide 1.60 and spectra generated from acceleration-time history.

an acceleration time-history developed from the Guide 1.60 spectra was used as input for the time-history analysis.

We believe the time-history method of analysis should be used as a standard for comparison. This method is the most accurate when a known acceleration time-history is used as input.

These results can be explained as follows:

Static Method

Static results are low since the structure was assumed rigid (T <0.05 sec) and no dynamic amplification was admitted. The actual model analyzed has a calculated fundamental period of T = 0.106 sec.

In an attempt to account for dynamic amplification, we examined the response spectra in Guide 1.60 for 5% damping and found a dynamic amplification of approximately three occurs for this model. This approach requires that the fundamental period be estimated or assumed. Three times the static results overestimates the response predicted by dynamic analysis. This difference is due to

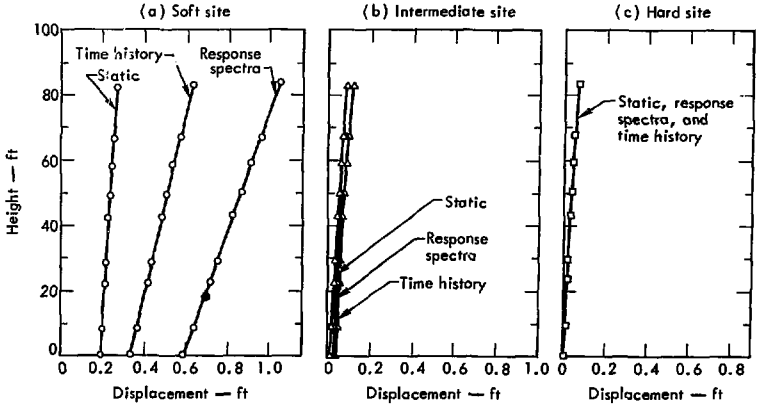

Fig. 30. Displacement calculations using three methods.

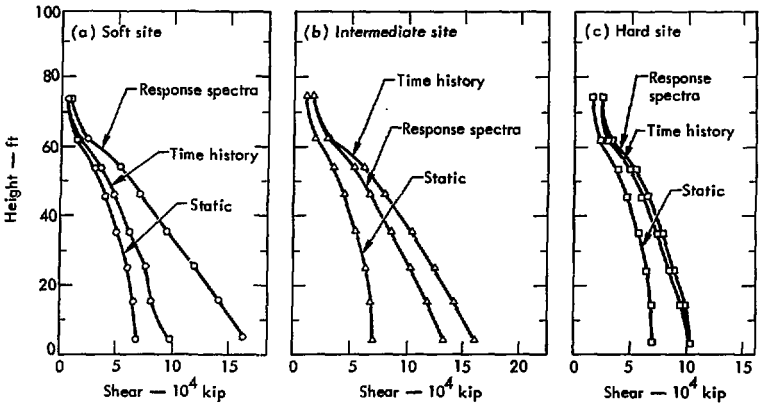

Fig. 31. Shear calculations using three methods.

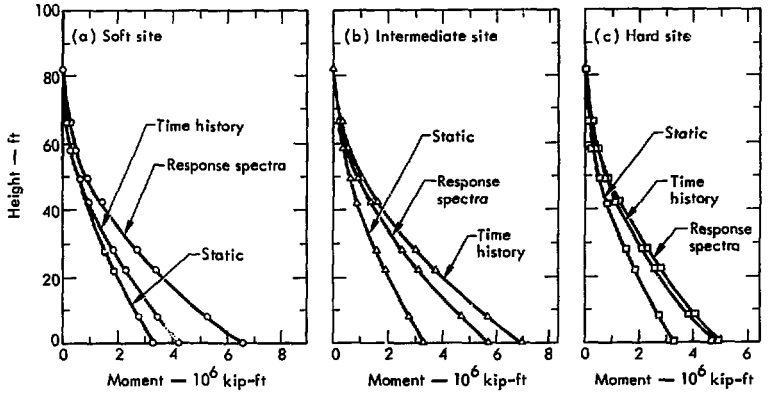

Fig. 32. *Moment calculations using* three methods.

difference in deformed shapes associated with the two approaches.

In summary, if we use an equivalent-static method of analysis, we generally get results lower than those obtained by dynamic analysis. To improve the results without becoming too conservative requires an estimate of the fundamental

period of the structure. The major advantage of the equivalent-static method is the ease with which the analysis can be conducted. However, the method produces low results and does not include site characteristics. The effort and uncertainty involved in improving the results do not appear justified when a dynamic analysis by response-spectra techniques can readily be conducted.

Time-History Method

The results from the time-history analysis are the most accurate for an input ground motion. The major disadvantages of this method are the large amount of computer time required to obtain a solution and the uncertainty in the input base acceleration time-history. Our input record was generated from Guide 1.60 and is an input record with the required frequency content. However, this record is not unique and many other records could also have the same frequency content as specified in Guide 1.60. Time-history analyses with other acceleration time-history records that conform to Guide 1.60 would result in different structural response.

Response Spectra Method

Results obtained by the response spectra method generally are largest of all three methods. This probably results from both the way in which the modal results are combined and the specification of input motion by a spectrum. This spectrum was developed to include the effects of many different earthquake acceleration time-histories and it represents an upper bound on the expected input seismic excitation.

The major disadvantage of this method is that acceleration time-histories at different elevations of the structure cannot be obtained. This information is required to produce floor spectra for designing equipment located within the structure. In addition, if more than one mode is important the absolute summing always yields conservative results and the SRSS summing may be conservative or non-conservative depending on period spacing of modes.

MANPOWER AND COMPUTER EFFORT

Table 10 indicates the manpower and computer effort requirements to develop seismic loads using the different types of analysis for structures founded at or near grade. Once these loads are defined, the designer would distribute them to the appropriate structural elements. The effort required for this task would be the same for all three methods and is not included in Table 11. We assume the structure to be of equal complexity to that of the Process Building. Three different site characterizations are assumed. Both horizontal directions are included in the estimate.

The values shown in the table represent upper limits. The actual effort will be dictated by the experience of the designer with structural analysis techniques and

Table 11. Manpower and computer effort-Process Building.

Method	Manpower (weeks)	Computer time (CDC 7600-min.)
Equivalent static	≤1	0
Response spectra	≤1.5	≤2
Time-history	≤3	≤5

computer application. The values include time required for development of a mathematical model, the generation of input forcing functions, computer interaction, and the interpretation of results.

CONCLUSIONS

We recommend the response spectrum method of analysis for structures founded near or at grade. The results show that the response spectrum method produces conservative results for relatively minimal manpower and computer efforts. This method adequately captures the important dynamic properties of the structure, can include site characteristics, and does not require an acceleration time-history record for input. Structural analysis is rapid and inexpensive to conduct with this method.

If a time-history of response quantities is required, the mode-superposition approach with a few modes included will produce the most economical results for at-grade structures similar to the Process Building. Time-history analyses will be more complex and time-consuming to perform than response spectra analyses.

The static method of analysis is suitable only for preliminary design of a structure like the Process Building. This analysis is easy and rapid to conduct, but the uncertainties associated with the results cannot easily be evaluated

Waste Tank Cell (WTC)

INTRODUCTION

Three methods exist for determining the earthquake design loads of fully buried structures: the equivalent-static method, dynamic analysis with a lumped-mass model, and dynamic analysis with a finite element model. We have compared the effectiveness of these approaches as applied to fully buried structures in fuel reprocessing plants.

To accomplish this, we selected the Waste Tank Cell (WTC) structure to be representative of fully buried structures at future reprocessing plants. We then calculated earthquake loading on the WTC resulting from vertical and horizontal ground motions with each of the three methods and compared the results. The comparison is based on technical and economic considerations. The former includes the accuracy of the computed design loads; the latter, man-hours and computer time required.

Vertical earthquake forces will principally affect the design of the upper and lower plates of the WTC. Horizontal earthquake loading will establish the design of the cylindrical shell. Since the WTC selected has a vertical axis of symmetry, only one horizontal component was considered. We also examined the effect of various possible site conditions (hard, intermediate, and soft) on the calculated loads.

Future WTC's will house a stainless steel tank that contains the radioactive liquid. We therefore considered the effect of the tank and possible sloshing on earthquake design loads. In the vertical analysis, the estimated mass of the tank plus the mass of the contained fluid (with

the tank assumed full) was distributed uniformly over the WTC foundation slab. In the horizontal analysis, the same procedure was used with a lesser amount of fluid. The smaller amount of fluid reflected the fact that a portion of it would not participate in the horizontal motion to any extent.

All three approaches assume that the soil and structural material properties are homogeneous, isotropic, and linear elastic and that damping is of the viscous type. In the finite element analysis, we also assume that static overburden pressure is sufficiently large to permit linear response even though the calculated

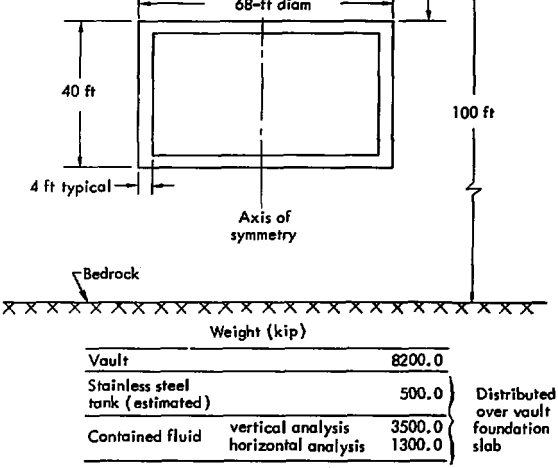

Weight (kip)

Vault		8200.0	
Stainless steel tank (estimated)		500.0	Distributed over vault foundation slab
Contained fluid	vertical analysis	3500.0	
	horizontal analysis	1300.0	

Materiol properties[a]

	γ Weight density (lb/ft^3)	C_s Shear wave velocity (ft/sec)	ν Poisson's ratio	E Young's modulus (10^6 lb/ft^2)	G Shear modulus (10^6 lb/ft^2)
Concrete	150.0	——	0.20	525.0	219.0
Soft soil	125.0	500.0	0.30	2.53	0.97
Intermediate soil	125.0	2000.0	0.30	40.4	15.5
Hard soil	125.0	4000.0	0.30	162.0	62.2

[a]Damping is assumed to be a uniform 7% of critical damping for the entire soil-structure system.

Fig. 33. Geometry, weight, and material properties of the WTC model.

results give rise to dynamic tensile soil stresses.

MODEL DESCRIPTION

The WTC is a completely enclosed concrete cylinder housing a stainless steel tank filled with liquid radioactive waste. The tank rests on a foundation slab. Figure 33 gives a detailed description of the geometry, mass, and material properties of the WTC used to develop our calculational models. There are some slight differences between the WTC design we used and the actual WTC at the Barnwell plant, none of which should significantly affect the comparison of results.

The top of the WTC was selected to be 10 ft below the ground surface. This burial depth is consistent with shielding requirements. The depth from the ground surface to the bedrock or hard soil media was selected to be 100 ft.

The actual WTC complex at Barnwell is a group of four closely spaced structures. Interaction among them may be important. However, we assume the WTC to be isolated for our analysis.

METHODS OF ANALYSIS

Equivalent-Static Analysis

Vertical Direction

Figure 34 shows the assumed load distribution on the WTC from vertical earthquake forces. The loading is divided into two parts: (1) those loads resulting from the weight of the top plate, and (2) those loads resulting from soil pressure acting on the tank. The plate contribution is assumed equal to the weight of the upper plate multiplied by the peak vertical ground acceleration. Along the upper plate the soil loading is set equal to the vertical overburden soil pressure multiplied by the peak vertical ground acceleration.

Along the cylindrical portion of the WTC, a lateral pressure is set equal to the overburden soil pressure multiplied

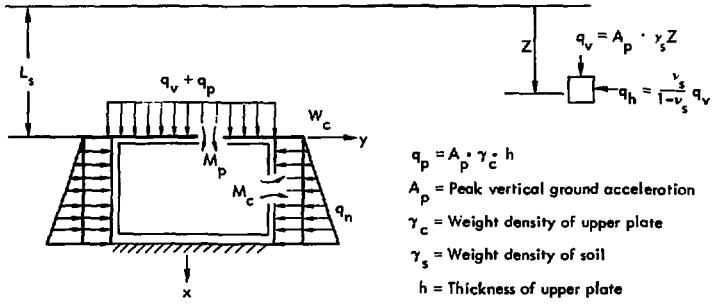

$q_p = A_p \cdot \gamma_c \cdot h$

A_p = Peak vertical ground acceleration

γ_c = Weight density of upper plate

γ_s = Weight density of soil

h = Thickness of upper plate

ν_s = Poisson's ratio of soil

z = Depth

Fig. 34. Vertical loading—static analysis.

both by the peak vertical ground acceleration and by $\nu_s/1 - \nu_s$, where ν_s is Poisson's ratio of the soil. This latter term reflects plane-strain considerations and may be considered a soil-pressure coefficient. The smaller the values of ν_s, the smaller is the effect of soil pressure acting on the WTC. In the vertical earthquake analysis, ν_s is taken to be one-half for simplicity and conservatism.

We assume that the tank is supported along its bottom and that the loading effects on the cylindrical shell at the junction of the side wall and upper and lower plates disappear rapidly as the distance from the edge increases. Thus, the solutions for the upper plate, the cylindrical side wall, and the lower plate for the loadings on the upper plate and lower plate are uncoupled. The loading effects of the upper plate and the lower plate on the WTC can be considered separately. We consider only the loading on the upper plate.

Because of the availability and the simplicity of the solutions, the loadings for the vertical static analysis are divided into two parts:

(1) The weight of the upper plate and the linearly varying soil pressure along the cylindrical shell.

The solutions for the moment and the deflection along the upper plate and cylindrical portion of the WTC are available in Flügge[16] and Timoshenko and Woinowsky-Krieger.[17] Their results using appropriate properties of the WTC, are summarized in Figs. 35 and 36. The deflection and the moment for the upper plate are denoted by $(W_p)_a$ and $(M_p)_a$. The deflection and the moment for the cylindrical shell are denoted by $(W_c)_a$ and $(M_c)_a$.

(2) The soil pressure acting on the WTC.

Thin plate and shell theory is used to develop the deflection and moment of the upper plate and cylindrical shell. The results are also summarized in Figs 35 and 36. The deflection and moment for the upper plate are denoted by $(W_p)_b$ and $(M_p)_b$. The deflection and moment for the cylindrical shell are denoted by $(W_c)_b$ and $(M_c)_b$.

The curves shown in Figs. 35 and 36 are based on the material and geometry properties of the WTC, the material properties of the surrounding soil, and the 1-g maximum earthquake vertical ground acceleration. Note that these curves are site independent because the only site characteristic in the model is the soil density and soil density is the same for hard, intermediate, and soft sites. Note also that the same scales are employed for comparing the magnitudes of the deflection and the moment.

Horizontal Direction

Figure 37 shows the model used to develop the static horizontal earthquake loading on the WTC. The exciting force is assumed equal to the weight of the upper plate plus the weight of the soil column directly above the tank. This magnitude of load represents a force equivalent to a 1-g maximum horizontal ground motion. For other values we can simply scale the results.

The resisting or restoring forces reflect the stiffness of the surrounding soil media and are represented by K_c (the compressive resistance), K_s (the shear resistance), and K_ϕ (the rocking

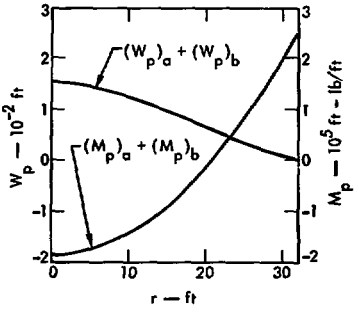

$$(W_p)_a = \frac{M_o(a^2 - r^2)}{2D(1+\nu)} + \frac{\gamma_c h(a^2 - r^2)}{64D}\left[\frac{5+\nu}{1+\nu}a^2 - r^2\right]$$

$$(M_p)_a = M_o + \frac{\gamma_c h(3+\nu)}{16}(a^2 - r^2)$$

$$(W_p)_b = \frac{-\gamma_s L_s}{64D}(r^4 - a^4) + \frac{1}{4}c_3(r^2 - a^2)$$

$$(M_p)_b = D\left[\frac{\gamma_s L_s}{16D}(3+\nu) - \frac{1}{2}c_1(1+\nu)\right]$$

$$M_o = \left[\frac{\gamma_c h a^3}{8(1-\nu)} - \frac{\gamma_s a^2}{(1-\nu^2)}\right] \Big/ \left(\frac{1}{2\kappa} + \frac{1}{1+\nu}\right)$$

$$D = Eh^3/12(1-\nu^2)$$

$$\kappa = \left[3(1-\nu^2)\frac{a^2}{h^2}\right]^{1/4}$$

$$c_1 = -\frac{\gamma_s L_s}{Eh}\left[1 - \frac{\nu}{2}\right]$$

$$c_3 = -\frac{4\kappa^2 c_2}{a^2(1+\nu)} - \frac{\gamma_s L_s a^2}{8D} - \frac{(3+\nu)}{1+\nu}$$

γ_c = Weight density of the concrete
γ_s = Weight density of the soil
a = Radius of the WTC
E = Young's modulus of the concrete
ν = Poisson's ratio of the concrete
L_s = The depth of the ground surface to the upper plate
h = The thickness of the WTC

Fig. 35. The deflection and the moment of the upper plate-static vertical analysis.

resistance). In the case of the compression spring, K_c, we used the vertical spring equation developed in the section on methods of analysis for rectangular foundations and considered the horizontal projection of the waste tank as the effective resistive area. Thus, B and L are the height and the diameter of the waste tank.

The deflections and spring forces can be determined by establishing horizontal equilibrium. Figure 38 gives the deflections and moment along the cylindrical

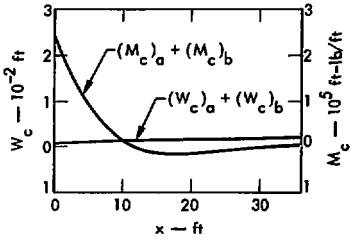

$$(W_c)_a = \frac{\gamma_c h a^4}{8kD(2\kappa+(1+\nu))} e^{-\frac{\kappa x}{a}} \sin\frac{\kappa x}{a} - \frac{\gamma_s a^3}{K(1-\nu^2)}\left[\frac{x}{a} - \frac{1+\nu}{2\kappa+(1+\nu)}\frac{1}{\kappa} e^{-\frac{\kappa x}{a}} \sin\frac{\kappa x}{a}\right]$$

$$(M_c)_a = \left[\frac{\gamma_c h a^2}{4} - \frac{2\gamma_s aD}{\kappa(1-\nu)}\right]\frac{(-\kappa)}{2\kappa+1+\nu} e^{-\frac{\kappa x}{a}} \cos\frac{\kappa x}{a} \qquad D = Eh^3/12(1-\nu^2)$$

$$(W_c)_b = \left(c_1 \cos\frac{\kappa x}{a} + c_2 \sin\frac{\kappa x}{a}\right) e^{-\frac{\kappa x}{a}} \qquad \kappa = \left[3(1-\nu^2)\frac{a^2}{h^2}\right]^{1/4}$$

$$(M_c)_b = \frac{-2D\kappa^2}{a^2}\left(c_1 \sin\frac{\kappa x}{a} + c_2 \cos\frac{\kappa x}{a}\right) e^{-\frac{\kappa x}{a}} \qquad c_1 = -\frac{\gamma_s L_s}{Eh}\left[1 - \frac{\nu}{2}\right]$$

$$c_2 = -\gamma_s L_s a^2 \left[\frac{a^2}{8kD(1+\nu)} + \frac{2-\nu}{2Eh}\right] \Big/ \left(1 + \frac{2\kappa}{1+\nu}\right)$$

γ_c = Weight density of the concrete
γ_s = Weight density of the soil
a = Radius of the WTC
E = Young's modulus of the concrete
ν = Poisson's ratio of the concrete
L_s = The depth of the ground surface to the upper plate
h = The thickness of the WTC

Fig. 36. The deflection and the moment of the cylindrical shell-static vertical analysis.

portion. Note that the deflection was derived for the soft site characteristics. For the intermediate and hard sites, values can simply be scaled by the factors 16 and 64, respectively. These factors reflect ratios of the different shear moduli of the soil.

Dynamic Analysis With Lumped Mass Model

Vertical Direction

Figure 39 shows the lumped mass model used for the WTC subjected to vertical ground motion. M_{p+s} is the generalized mass of the upper plate and

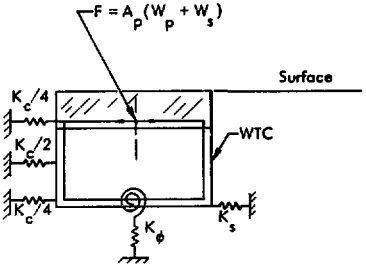

W_s = Weight of soil column
W_p = Weight of upper plate
A_p = Peak horizontal ground acceleration
K_c = Soil compressive resistance
K_s = Soil shear resistance
K_ϕ = Soil rotational resistance

Fig. 37. Horizontal loading – static analysis.

the soil column above the WTC. The stiffness of the waste tank structure itself is captured with the generalized spring constant, K_p, which models the bending stiffness of the upper plate. The generalized mass and the generalized spring constant for the upper plate are derived by considering the flexural characteristic of the upper plate, assumed to be a uniformly loaded, clamped, circular plate. M_{c+p+l} is the mass of the cylindrical shell, the lower plate, and the waste tank internals. The soil column is not included in the generalized mass of the upper plate. K_c and K_s reflect the compressive and shear resistance provided by the surrounding soil and are defined in the section on methods of analysis.

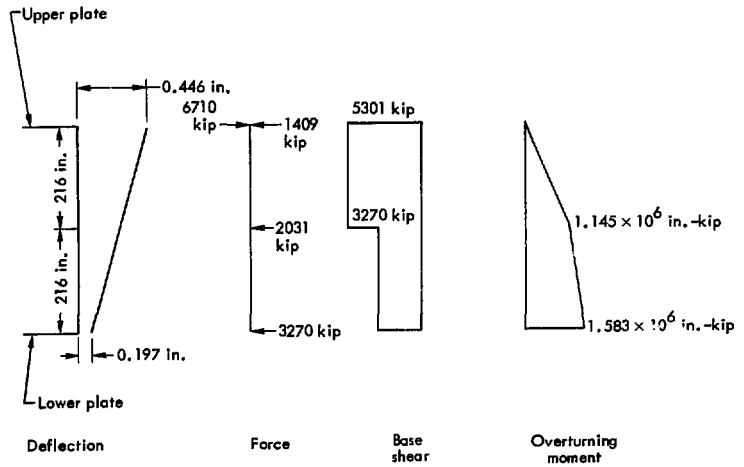

Fig. 38. Deflection, shear force, and bending moment diagrams for static horizontal analysis.

This two-degree of freedom lumped mass system was solved with the SAPIV computer program. The 7% damping horizontal response spectrum shown in Fig. 7 was used directly as input. Table 12 summarizes the results. Calculations include hard, intermediate, and soft site characteristics. The geometry and material properties shown in Fig. 33 were used.

The moment in the upper plate is shown in Fig. 40. This moment is calculated from the maximum deflection of the upper plate, which is taken to be the difference between the deflections of mass M_{c+p+I} and the mass M_{p+s}.

Horizontal Direction

The lumped mass model developed to analyze the horizontal response of the

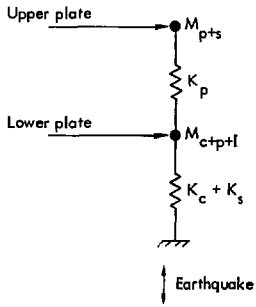

K_p = Spring reflecting bending stiffness of upper plate
K_c = Soil compressive resistance
K_s = Soil shear resistance
M_{p+s} = Generalized mass of upper plate plus soil column above tank
M_{c+p+I} = Mass of cylindrical shell plus lower plate plus waste tank internals.

Fig. 39. Lumped mass vertical model.

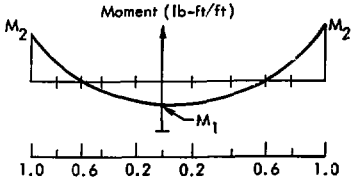

Site	Moment at center (M_1)	Moment at edge (M_2)
Soft	-2.474×10^5	4.138×10^5
Inter-mediate	-2.228×10^5	3.726×10^5
Hard	-1.479×10^5	2.926×10^5

Fig. 40. Moment upper plate – lumped mass vertical analysis.

WTC is shown in Fig. 41. M_{p+s} represents the mass of the upper plate plus the mass of the soil column above the tank. M_c is the mass of cylindrical portion of the tank, and M_{p+I} is equal to the mass of the lower plate plus the mass of the internal equipment plus approximately the mass of liquid waste in the WTC. K_s, K_c, and K_ϕ reflect the shear, compressive, and rotational resistance provided by the soil. These springs were the same spring constants used in the static horizontal analysis.

As with the vertical direction, this lumped mass model was solved with the SAPIV computer program. The 7%

Table 12. Lumped mass vertical response analysis results – WTC.

Site	Frequency (cps) 1st mode	Frequency (cps) 2nd mode	Deflection (in.) $\Delta_{M_{p+s}}$	Deflection (in.) $\Delta_{M_{c+p+I}}$
Soft	4.5	12.0	1.39	1.17
Intermediate	11.2	19.3	0.23	0.04
Hard	11.4	38.0	0.16	0.01

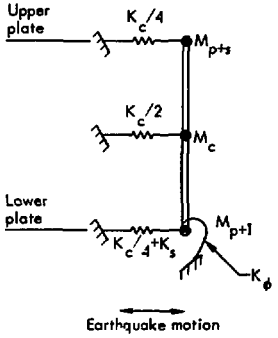

K_ϕ = Soil rotational spring
K_c = Soil compressive spring
K_s = Soil shear spring
M_{p+s} = Mass of upper plate plus soil column above tank
M_c = Mass of cylindrical portion of tank
M_{p+l} = Mass of lower plate plus tank internals

Fig. 41. Lumped mass horizontal model.

damping horizontal response spectrum shown in Fig. 7 was used as input. Calculations include hard, intermediate, and soft site considerations. Figure 33 geometry and material properties were used. Table 13 summarizes the results. Note that the maximum moment and the maximum shear force are the total maximum bending moment and the total maximum shear force in the cylindrical side wall.

Dynamic Analysis With Finite Element Model

The finite element model used is shown in Fig. 42. The diameter of the soil region modeled is 320 ft. Depth to bedrock was selected as 100 ft. The WTC was represented by shell elements. The surrounding soil is represented by solid elements. The solid finite elements used are 8 ft horizontally and 4 ft vertically.

The model was the same for both the vertical and horizontal analyses with two exceptions. First, for the vertical analyses, radial (or lateral) motion was not permitted along the vertical boundary of the mode; for the horizontal analysis, vertical motion was restrained along this

Table 13. Lumped mass horizontal response results— WTC.

		Site condition		
		Soft	Intermediate	Hard
Modal frequencies (Hz)	1st	4.5	17.3	32.2
	2nd	9.9	33.9	55.5
	3rd	74.1	76.1	83.2
Displacements (in.)	Top	1.47	0.062	0.013
	Mid-cylinder	1.20	0.046	0.008
	Bottom	0.93	0.031	0.004
Displacement at top relative to bottom (in.)		0.55	0.031	0.010
Base shear (10^6-lb)	Top	5.38	3.20	2.14
	Bottom	8.36	4.62	2.32
Overturning moment (10^6 ft-.b)	Top	0.0	0.0	0.0
	Mid-cylinder	97.0	58.0	39.0
	Bottom	247.0	140.0	78.0

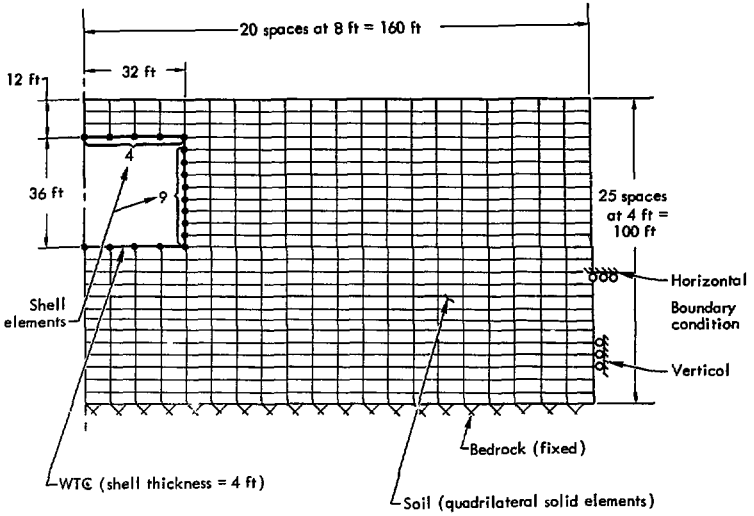

Fig. 42. Finite element mesh of WTC. (Fig. 33 gives soil and shell element material properties.)

boundary. Second, for the vertical analysis, the stainless steel tank was assumed to be filled with liquid waste. The mass of the tank and the liquid waste is evenly distributed along the lower plate; for horizontal analysis, a smaller amount of the mass was distributed to account for possible sloshing of the liquid waste in the tank. The actual physical properties of the WTC and the surrounding soil as well as the weight of the stainless steel tank are shown in Fig. 33.

Figures 43 and 44 indicate the fundamental mode shapes and frequencies obtained by GHOSH.[15] Also included for comparison are predicted results obtained from a closed-form solution. This solution develops the characteristic frequencies and mode shapes for the equations of motion for shear response of a homogenous, isotropic, plane strain, elastic continuum. The frequency equation for an infinite site is

$$f_k = \frac{(2k - 1)\, C}{4\, h},$$

where

C = compressional wave speed for vertical site mode or shear wave speed for horizontal site mode

h = 100 ft (site depth)

k = 1 for lowest free-field site mode.

The fact that the finite element frequencies agree very well with those predicted indicates that the outer boundary of the

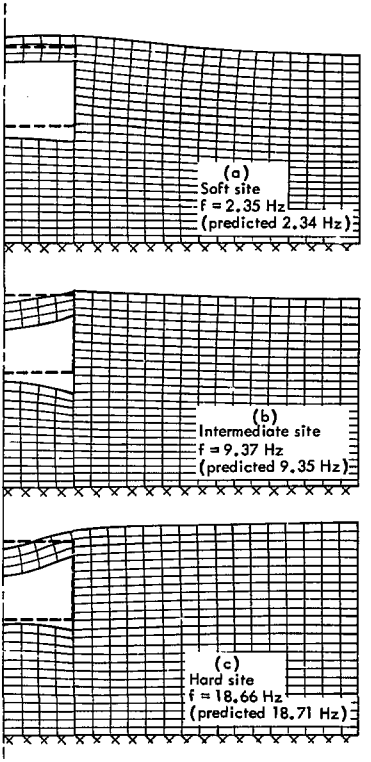

Fig. 43. Mode shapes and frequencies of fundamental vertical modes.

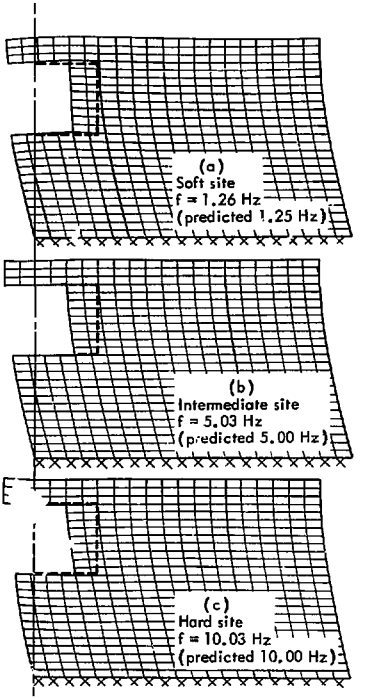

Fig. 44. Mode shapes and frequencies of fundamental horizontal modes.

soil is sufficiently far from the structure. The closed-form solution also predicts that the displacement distribution through the depth at free-field is a quarter-sine wave, being maximum at the surface and zero at bedrock. Both the vertical and horizontal mode shapes agree with this very well at the outer boundary.

The results of the vertical analysis were surprising in one way. Due to the shallow layer of soil over the WTC, we expected to see the primary mode shape involving vertical vibration of the roof at a frequency of approximately 11 Hz.* In the intermediate and hard soil mode shapes

*Based on a handbook solution for a clamped plate that includes the mass of the overhead soil.

(see Fig. 43), the upper plate mode is present and is combined with the fundamental system mode. This is possible in the intermediate soil model because the roof and system frequencies are quite close. The stiffer soil in the hard soil model drives the roof frequency upward so that the combined mode at 18.66 Hz is feasible.

For the soft soil vertical case, we did not observe any upper plate participation in the fundamental mode. We feel that the soft site results require a more detailed investigation. For this reason, the deflections and loads presented in Fig. 43 for the vertical soft soil case must be used with caution.

Figure 45 indicates some key relative displacements for the six cases analyzed. In effect, it quantifies the mode shapes given earlier. These displacements provide a basis for comparison to the other methods of analysis and give the reader a better

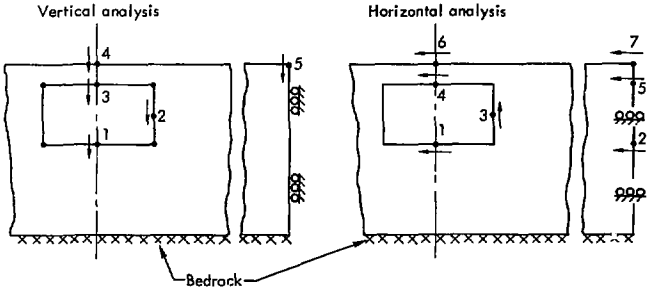

Soil condition		Vertical analysis Soft	Intermediate	Hard	Horizontal analysis Soft	Intermediate	Hard
Fundamental site frequency (Hz)		2.35	7.37	18.66	1.26	5.03	10.03
Spectral acceleration applied at bedrock[a] (g)		1.86	2.23	1.44	1.56	2.46	2.11
Displacements relative to bedrock (in.)	1	≥ 1.53	0.084	0.020	9.50	0.836	0.161
	2	≥ 2.06	0.217	0.058	9.04	0.888	0.188
	3	≥ 2.17	0.360	0.150	1.31	0.013	-0.017
	4	≥ 2.23	0.356	0.146	10.96	1.17	0.275
	5	≥ 4.72	0.339	0.045	12.14	1.19	0.258
	6	——	——	——	11.53	1.19	0.270
	7	——	——	——	12.36	1.22	0.263

[a]These values ore from Figs. 6 and 8 and correspond to the fundamental site frequencies.

Fig. 45. Results of WTC finite element analysis – fundamental site frequencies, spectral accelerations, and relative displacements.

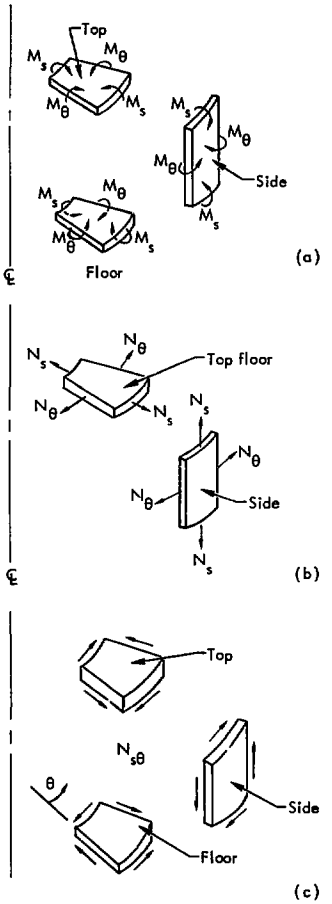

Fig. 46. Definitions and sign conventions of stress-resultants. (a) M_s and M_θ are the stress-resultant moments. Units are (ft-lb/ft). A positive value produces tension on the inside of the WTC as shown. (b) N_s and N_θ are the stress-resultant forces. Units are (lb/ft). Positive value produces tension. (c) $N_{s\theta}$ is the stress-resultant in-plane shear force. Units are (lb/ft). Positive as shown.

understanding of what ground motion does to the WTC.

Figure 46 defines the sign convention and stress resultants used. Figures 47 and 48 give plots of the stress-resultant shell loads in the WTC for vertical and horizontal ground motion. The sign convention is in agreement with the relative displacements given earlier in Fig. 45. To facilitate a comparison with lumped mass horizontal analysis, the overturning moment and shear along the cylindrical part of the WTC was calculated from the shell forces mentioned above. These overall "body-bending" forces are presented in Fig. 49.

COMPARISON OF METHODS

To compare results from three models analyzed (equivalent-static, lumped mass, and the finite element), we selected several response parameters of the WTC. The comparison demonstrates the variation in results from the vertical and horizontal analyses and permits us to draw conclusions about the choice of method for the seismic response evaluation of fully buried structures, particularly future WTC's that have the characteristics modeled.

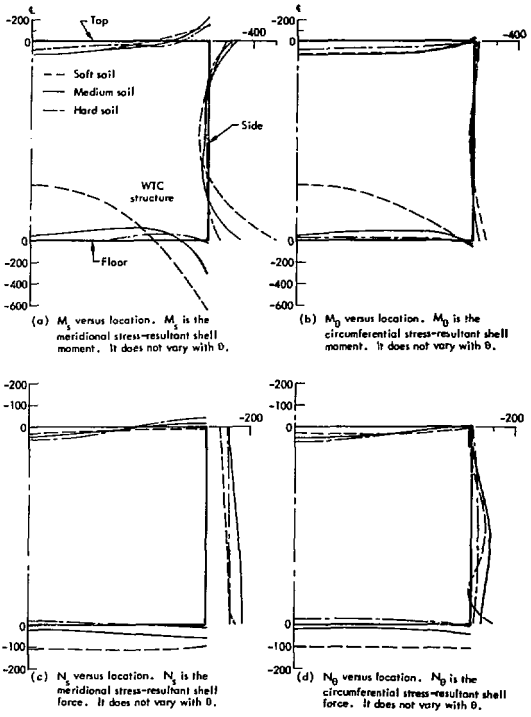

Fig. 47. WTC vertical finite element analysis. Distribution is axisymmetric. RG160 vertical spectrum applied at bedrock, 7% damping, normalized to 1 g maximum ground acceleration.

Vertical Analysis

For the vertical case, we have selected moment and deflection quantities to identify the variation in results from the three methods. Figure 50 and Table 14 summarize these comparisons. Figure 50 shows the moment distribution in the upper plate and the cylindrical sides of the waste tank for all three models for hard, intermediate, and soft sites. Table 14 gives numerical values of deflection as well as the maximum moments. Below we list some observations regarding the variation in results:

(1) All three methods produced moment diagrams that have basically the same shape.

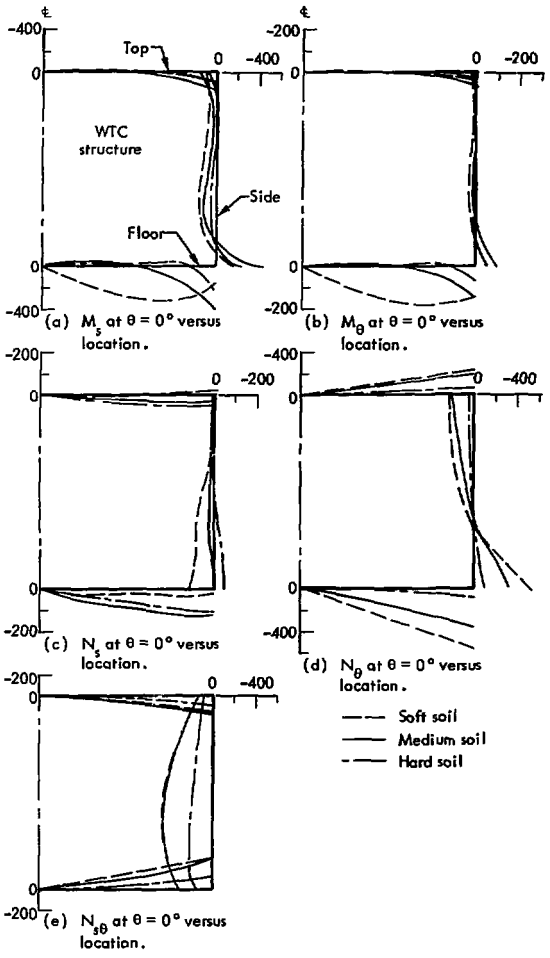

Fig. 48. WTC horizontal finite element analysis. Terms are as defined on Fig. 47, except the shell moment varies circumferentially as the cos θ. For (e), $N_{s\theta}$ is the meridional circumferential shear stress-resultant. $N_{s\theta}$ acts in the plane of shell RG160 horizontal spectrum applied at bedrock, 7% damping, normalized to 1 g maximum ground acceleration.

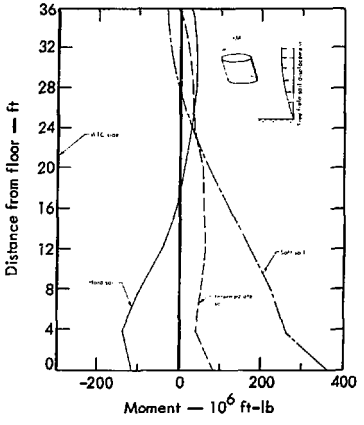

Fig. 49. WTC horizontal finite element analysis overturning moment in cylindrical shell versus distance up from bottom plate.

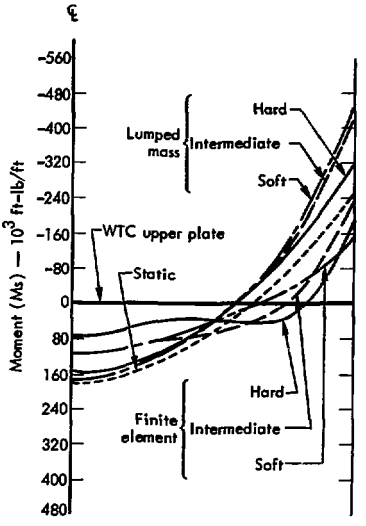

Fig. 50. Comparison of results – vertical analysis WTC.

Table 14. Comparison of results – vertical analysis WTC.

Item	Site	Static	Lumped mass	Finite element
Vertical deflection	Soft	0.18	0.22	≥0.11
Center top plate	Intermediate	0.18	0.23	0.14
Relative to shell	Hard	0.18	0.16	0.09
(in.)				
Moment	Soft	183.0	247.0	≥116.0
Center top plate	Intermediate	183.0	258.0	116.0
(10^3 ft-lb/ft)	Hard	183.0	155.0	76.0
Moment	Soft	245.0	414.0	≥147.0
Edge of top plate	Intermediate	245.0	431.0	232.0
(10^3 ft-lb/ft)	Hard	245.0	306.0	188.0

(2) All three methods produced maximum deflection of the upper plate and center and edge moments in the upper plate that are in reasonable agreement. The lumped mass results are the largest, the equivalent static intermediate, and finite element the smallest. The higher lumped mass values reflect the dynamic amplification from input ground motion. For example, at 11 Hz (the approximate fundamental frequency of the upper plate) the maximum ground motion of 1 g is amplified to approximately 1.7 g. Although the finite element method accounts for such amplification, the soil media contribution tends to increase the fundamental period of the systems such that a lesser amplification results. Our static method did not account for amplification, although proper selection of the g level coefficient would have allowed this factor to be included.

(3) The results show a considerable variation due to the different site stiffnesses. Maximum center upper plate deflections and plate and cylinder moments show a variation greater than 50% going from hard to intermediate soil stiffnesses.

(4) The static and lumped mass models reflected our judgment as to how the upper plate of the WTC responds to vertical seismic loading. The shell side wall loads were induced moments resulting from the continuity condition imposed at the upper plate and shell junction. Neither reflected effects from the lower plate. The finite element analysis automatically includes the stiffness characteristics of the entire WTC structure plus soil-structure effects in distributing the loads. The finite element analysis shows bottom plate moments that are much greater than the upper plate for soft sites. Thus, assumptions implicit in our static and lumped mass analysis proved to be correct for the hard and intermediate sites. For the soft site they were not. This discrepancy points to the need for an a priori good understanding of the response when using the static and lumped mass methods.

(5) Local soil conditions play a major role in determining WTC stresses. The finite element methods results show that the resistive load paths to the seismic motions change with soil stiffness. For example, for intermediate and hard sites, vertical loads are transferred primarily into the soil media by shear transfer along the shell of the waste tank. For the soft site, the loads are transferred by a distributed normal pressure along the lower plate (see the large moment in the lower plate in Fig. 50. Our static analysis did not account for this. The lumped mass did (although results are not plotted on Fig. 50). Both static and lumped mass methods could include soil stiffness springs to account for such possibilities, but not without increasing the complexity of the models, particularly the selection of appropriate spring constants.

Horizontal Analysis

For the horizontal case, we have selected the overturning moment, and shear and horizontal deflections as response characteristics to compare the

variation in the results from the three methods. Figure 51 plots overturning versus height above base of the WTC. These values were obtained from equilibrium consideration for the static and lumped mass analyses. For the finite element analysis, it was necessary to integrate the shell moment (M_s) plus the shell axial stress (N_s) over 360° to get the overturning moment. Table 15 gives the absolute horizontal displacement at the top and bottom of the WTC, the relative horizontal displacements between the top and bottom, and overturning moment and shear at top and bottom. Variations in results because of different site characterization (i.e., hard, intermediate, soft) are also included in both Fig. 51 and Table 15. Some observations on the variation in calculated results follow:

(1) The static method produced smaller absolute horizontal displacements at both the top and bottom plates than the lumped mass approach, by as much as a factor of four. Relative deflections calculated by the static analysis was also smaller than the lumped mass, by a factor of two. The static and lumped mass analyses both used the same set of soil springs. The geometrical arrangement of the springs was also the same. The difference noted in the calculated deflections arise from the inclusion of dynamic amplification and inertia forces in the lumped mass analysis.

(2) The finite element analysis produced absolute displacements (top and bottom of tank) and relative displacements larger than the static or lumped mass results by an order of magnitude. This difference results primarily because of the way the methods account for the site response characteristics. The finite element analysis indicates that site response dominates the motion of the WTC (see fundamental mode shapes in Figs. 43 and 44). Fundamental frequencies of the finite element system are 1.25, 5.03, and 10.03 Hz for the soft, intermediate, and hard sites. These are considerably different from 4.5, 16.3, and 32.2 Hz associated with the lumped mass analysis. Hence, we attribute these differences to amplification effects and the way the soil springs reflect the site deformation characteristics.

(3) A comparison of overturning shear at both the top and bottom of the WTC shows the static and lumped mass cases to be lower than the finite element values. There appears to be no

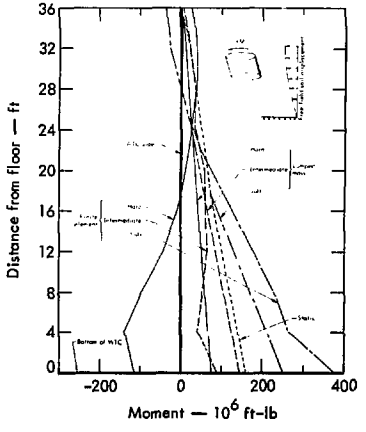

Fig. 51. Comparison of results—horizontal analysis WTC.

consistent relationship between values. The difference can be attributed primarily to site amplification differences and the way the lumped mass and finite element methods include the site characteristics.

(4) Note that the static results produce a loading on the WTC independent of site properties. Calculated deflections do consider site characteristics effects.

(5) The finite element results (see Fig. 48a) indicate that the bending stresses in the top and bottom plate are significant. Neither the static nor lumped mass models we used give these stresses directly. Simplified loading assumptions could be made such that we could develop top and bottom plate loading. However, the pressure distribution would require considerable refinement to models in order to include local soil characteristics.

MANPOWER AND COMPUTER EFFORT

The manpower and computer effort associated with analysis must be considered when evaluating different methods. Therefore, estimates of the effort required for each of the three WTC analysis are shown in Table 16. These estimates indicate the relative effort required for the three methods. We assume that the analyst is experienced with structural analysis techniques and computer analysis. The amount of experience in these areas will indicate the actual effort required.

The static and lumped mass estimates allow for developing and formulating a suitable model, interpreting results, remodeling (if necessary), and the analysis itself. Computer time required for these two methods is negligible compared to the finite element analysis.

The finite element estimate is for two analyses (vertical and horizontal) using a GHOSH-like computer program on a CDC 7600. The response spectra approach is assumed as well as an axisymmetric WTC-like structure. Allowance is made for additional complications such as important internal structures and varying soil properties (three sites).

CONCLUSIONS

The results of the WTC analysis strongly suggest that finite element techniques should be used to model fully buried structures similar to the WTC. Site amplification effects were shown to be important. Load transfer mechanisms were seen to be very much dependent on the relative stiffness between the WTC structure and local soil properties. Finite element techniques more directly consider all these effects. It is much more difficult to account for these items with static on lumped-mass models, and uncertainties associated with these models will be much greater than those with the finite element model. We recommend the use of the finite element method to model fully buried structures.

If time-history response quantities are required (e.g., to generate load definition for internal equipment) or if it is felt the analysis must incorporate strain compatible soil properties, then the time-history method of solution is necessary. If the time-history response and strain compatibilities are not required, then the response spectrum approach would be the most economical method of solution.

Table 15. Comparison of results – horizontal analysis WTC.

Item	Site	Static	Lumped mass	Finite element
Horizontal displacement (in.)	Soft	0.45	1.47	10.96
Top of WTC	Intermediate	0.03	0.06	1.17
Relative to bedrock	Hard	0.007	0.013	0.28
Horizontal displacement (in.)	Soft	0.20	0.930	9.50
Bottom of WTC	Intermediate	0.01	0.031	0.84
Relative to bedrock	Hard	0.003	0.004	0.16
Horizontal displacement (in.)	Soft	0.25	0.55	1.46
Top of WTC	Intermediate	0.02	0.03	0.33
Relative to bottom of WTC	Hard	0.004	0.01	0.11
Overturning moment (10^6 ft-lb)	Soft	0.0	0.0	34.0
Top of WTC	Intermediate	0.0	0.0	3.0
	Hard	0.0	0.0	29.0
Overturning moment (10^6 ft-lb)	Soft	154.0	247.0	376.0
Bottom of WTC	Intermediate	154.0	140.0	88.0
	Hard	154.0	78.0	117.0
Overturning shear (10^6 lb)	Soft	5.30	5.38	12.9
Top of WTC	Intermediate	5.30	3.30	19.1
	Hard	5.30	2.14	13.3
Overturning shear (10^6 lb)	Soft	3.27	8.36	29.3
Bottom of WTC	Intermediate	3.27	4.62	18.7
	Hard	3.27	2.32	3.8

Table 16. Manpower and computer effort – WTC.

Method	Manpower (weeks)	Computer time (CDC 7600-min.)
Equivalent-static	≤ 0.5	≤ 1
Lumped mass	≤ 1	≤ 1
Finite element	<3	≤ 30

Fuel Receiving and Storage Station (FRSS)

INTRODUCTION

Our objective is to compare three procedures for calculating seismic effects on deeply embedded structures. We used the Fuel Receiving and Storage Station (FRSS) as an example of a typical deeply embedded structure and calculated the seismic forces from horizontal ground motion. We used three models to make these calculations: static, lumped mass, and finite element.

All analyses assume linear elastic behavior. These analyses were limited to calculating only the seismic forces imposed on one embedded wall of the structure. The same procedures could be applied to all walls to determine design forces. We believe the walls could be designed statically once the seismic forces have been determined, so we limited this study to comparing various methods of determining seismically induced forces on deeply embedded structures.

All results were obtained for an earthquake with a maximum ground acceleration of 1 g that meets the criteria established in Guide 1.60 (Ref. 11). The 7% damped response spectrum shown in Figs. 8 and 9 was used. The effect of the site soil properties was also included in the comparison. Soft, intermediate, and hard sites were considered.

MODEL DESCRIPTION

The fuel receiving and storage station consists of two structures: the pool structure and the FRSS building. The pool structure is a series of contiguous buried pools for fuel handling. The FRSS building is a steel structure founded at grade that encloses the pool structure and supports the overhead cranes. The two are structually separate. This analysis is limited to the buried pool structure.

A typical view of pool structure is shown in Fig. 52. The structure consists of four main areas: the decontamination pit, the cast unloading pool, the fuel storage pool, and the fuel transfer pool. The cast unloading pool and the fuel transfer pool are 65 ft deep. All walls are 4 ft thick. The pool structure is reinforced concrete.

For our analysis we have simplified the pool structure to the buried structure shown in Fig. 53. Only seismic forces on exterior walls were considered. For this analysis the direction of earthquake shaking was assumed to be longitudinal. We computed seismic forces on the 75-ft by 65-ft end wall by various approaches and compared the results. Material properties for concrete and the three site properties used in this analysis are shown in Table 17.

METHODS OF ANALYSIS

We used four approaches to determine the dynamic pressure distribution on a typical wall. These are: (1) pressure distribution determined by the Mononobe-Okabe earth pressure theory[18]; (2) pressure distribution determined by assuming rigid structure on elastic half space; (3) pressure distribution determined from dynamic response of a lumped mass model of the pool structure; and (4) pressure distribution determined from a plane-strain finite element model of the

Table 17. Material properties.

	γ(lb/ft^3)	C_s Shear wave velocity (ft/sec)	ν Poisson's ratio	E Young's modulus (10^3 kip/ft^2)	G Shear modulus (10^3 kip/ft^2)
Concrete	150.0	–	0.20	525.0	219.0
Soft soil	125.0	500.0	0.30	2.53	0.97
Intermediate soil	125.0	2000.0	0.30	40.4	15.5
Hard soil	125.0	4000.0	0.30	162.0	62.2

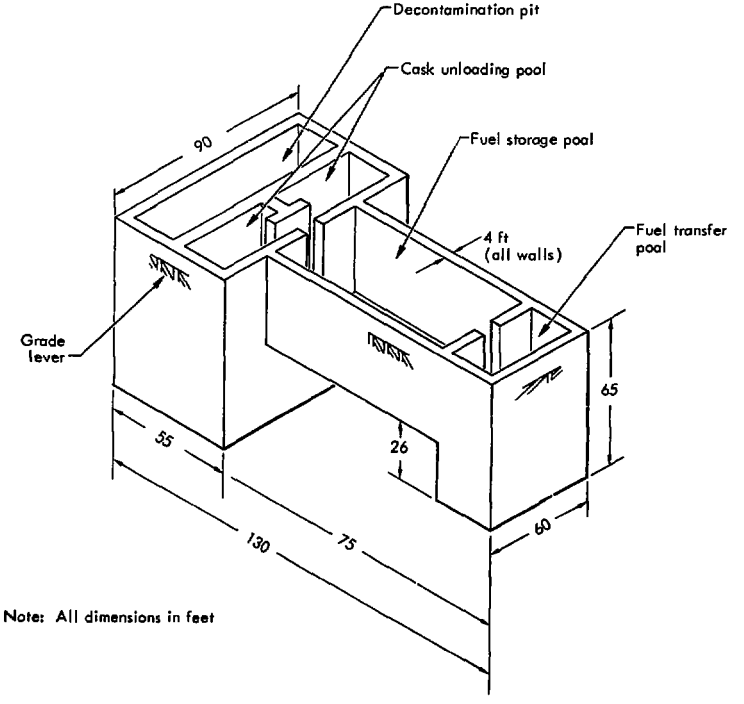

Fig. 52. Typical FRSS pool structure.

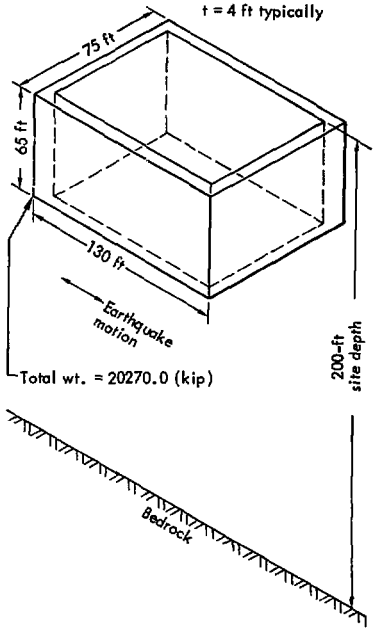

Fig. 53. Pool structure used for analysis.

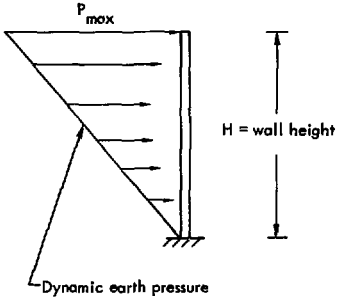

Fig. 54. M-O dynamic pressure distribution.

soil-structure system. The first two approaches are equivalent-static models; the third and fourth use lumped mass and finite element models, respectively.

Equivalent-Static Models

(1) A rapid estimate of the dynamic earth pressure acting on the pool structure wall can be obtained with the Mononobe-Okabe (M-O) earth pressure theory. This theory assumed a linearly varying pressure distribution as shown in Fig. 54. The maximum dynamic earth pressure can be determined from:

$$P_{max} = \gamma H \Delta K_{AE}, \quad (1)$$

where

γ = unit weight of soil

H = wall height

ΔK_{AE} = dynamic earth pressure coefficient = $\frac{3}{4}\frac{a}{g}$

a = maximum ground acceleration

g = acceleration of gravity.

This method of analysis does not include the effects of site stiffness.

(2) Another approach to determining the wall pressure distribution is to assume that the pool structure is rigid and the soil is an elastic material. The soil is represented as springs. The spring constants can be determined from the equations in the section on methods of analysis. Values of the spring constants for each site are listed in Table 18. The model used for this analysis is shown in Fig. 55. In this

analysis we imposed the displacements Δ_1, Δ_2, Δ_3, Δ_4 as shown. Values for these displacements were determined from the closed form solution for infinite elastic sites, as shown in the following:

$$\Delta_i = \frac{S_A}{\pi^3 f^2} \sin \frac{\pi h_i}{2D}, \qquad (2)$$

where

S_A = spectral acceleration at bedrock

h_i = distance to point of interest

D = depth to bedrock

f = frequency = $\frac{C_S}{4D}$

C_S = shear wave velocity in soil.

Figure 56 further defines terms. The values used for this analysis are listed in Table 19.

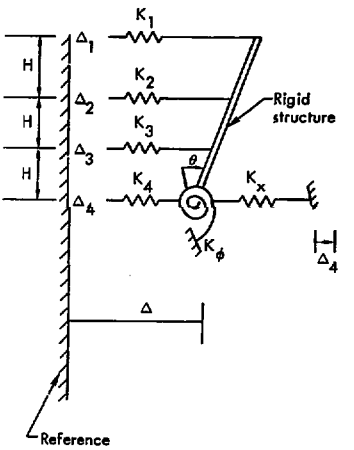

Known quantities

Δ_1, Δ_2, Δ_3, Δ_4

K_1, K_2, K_3, K_4, K_x, K_ϕ

H

Unknown quantities

Δ, θ

Fig. 55. Rigid model in elastic half-space.

Lumped Mass Model

The wall pressure distribution was also obtained by modeling the pool structure as series of lumped masses interconnected by shear beams. The effects of the soil are included as springs. The model used is shown in Fig. 57. Values for the mass and stiffness characteristics of the pool structure are shown in Table 20. This model was excited at all horizontal springs with the 7% damped response spectrum defined in Guide 1.60.

Finite Element Model

Wall pressure distributions were also estimated by constructing a finite element model of the soil-structure system. The model used for this analysis is shown in Fig. 58. The soil was represented as plane-strain solid finite elements, while the FRSS pool structure was modeled

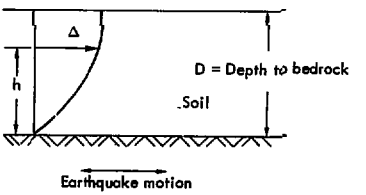

Fig. 56. Defining terms for Eq. (2).

Table 18. Spring constants for three sites.

Site	K_1 (10^6 kip/ft)	K_2 (10^6 kip/ft)	K_3 (10^6 kip/ft)	K_4 (10^6 kip/ft)	K_x (10^6 kip/ft)	K_ϕ ($\frac{10^{10}\ \text{kip-ft}}{\text{rad}}$)
Soft	0.03	0.05	0.05	0.03	0.24	0.10
Intermediate	0.40	0.79	0.79	0.40	3.78	1.60
Hard	1.57	3.14	3.14	1.57	15.17	6.42

Table 19. Imposed displacements for three sites.

Site	C_s (ft/sec)	f^a (H_z)	$S_A{}^b$ (ft/sec^2)	Δ_1 h = 200.0 (ft)	h = 178.3 (ft)	h = 156.67 (ft)	h = 135.0 (ft)
Soft	500.0	0.625	28.9	2.39	2.35	2.25	2.08
Intermediate	2000.0	2.50	87.5	0.451	0.445	0.425	0.39
Hard	4000.0	5.00	79.3	0.102	0.101	0.096	0.089

[a] f is based on 200 ft site depth.

[b] S_A is based on Guide 1.60. Horizontal spectra for 7% damping, normalized to 1 g maximum ground acceleration.

Table 20. Mass and stiffness characteristics of pool structure. (This model was excited at all horizontal springs with the 7% damped response spectra defined in Guide 1.60.)

Location	Mass (K-sec^2/ft)	Shear stiffness (10^6 kip/ft)
1	80	10.5
2	160	10.5
3	160	10.5
4	235	

$$\text{Shear stiffness} = \frac{A_s G}{L}$$

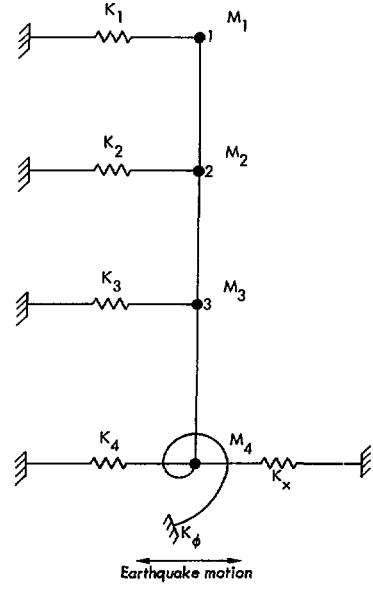

Fig. 57. Lumped mass model of FRSS pool structure-soil interaction.

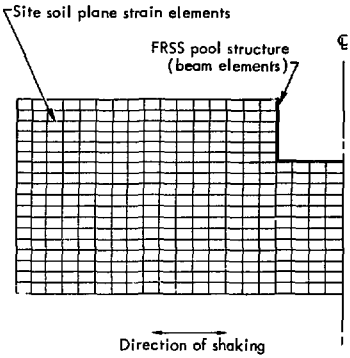

Fig. 58. Finite element model of FRSS pool structure – soil system.

with beam elements. The model was excited with the 7% damped horizontal spectrum from Guide 1.60 applied at the base level.

Soil properties were varied to study the effects of site characteristics. The stiffness of the pool structure was varied to study the effects of structure stiffness on the resulting wall pressure distribution.

COMPARISON OF METHODS

Figure 59 gives the earthquake-induced soil pressure distributions calculated by the four methods (*M-O, rigid structure* with imposed displacement, lumped mass, and finite element). A complete analysis of the FRSS pool structure would include the structure inertia forces and the forces due to shear at th soil-structure interface. For comparison purposes we considered only the soil pressure load because it is the most important earthquake load and because it is the only quantity calculated in the simpler methods. Figure 59 indicates that the soil pressure magnitude and distribution vary considerably with method, soil stiffness, and (in the case of the finite element analysis) rigidity of the structure.

The foundation soil pressure is computed in the three simplified methods by assuming that the overturning moment created by the lateral pressure is resisted by a linearly varying pressure on the foundation. Therefore the sign and distribution are identical for these three methods; only the magnitudes vary. The M-O and lumped mass methods predict peak foundation pressures between 1 and 3 kip/ft^2. The rigid-structure-with-imposed-displacements method predicts peaks of 3 to 11 kip/ft^2. These differences in foundation pressures are due to the differences in wall pressure distributions.

The finite element method makes no such assumption about the foundation pressure distribution. The overturning moment calculated by the finite element method was seen to be totally resisted by shear along the walls. Furthermore, in five of the six finite element cases, the overturning moment created by the foundation pressure was in the same direction as that created by the lateral pressure. The pressure magnitudes show considerable variation, depending upon soil and structure stiffness. The peaks range from 3 to 31 kip/ft^2. The important point here is that the finite element method predicts foundation pressures that are quite different in sign and magnitude from those predicted in the simpler methods.

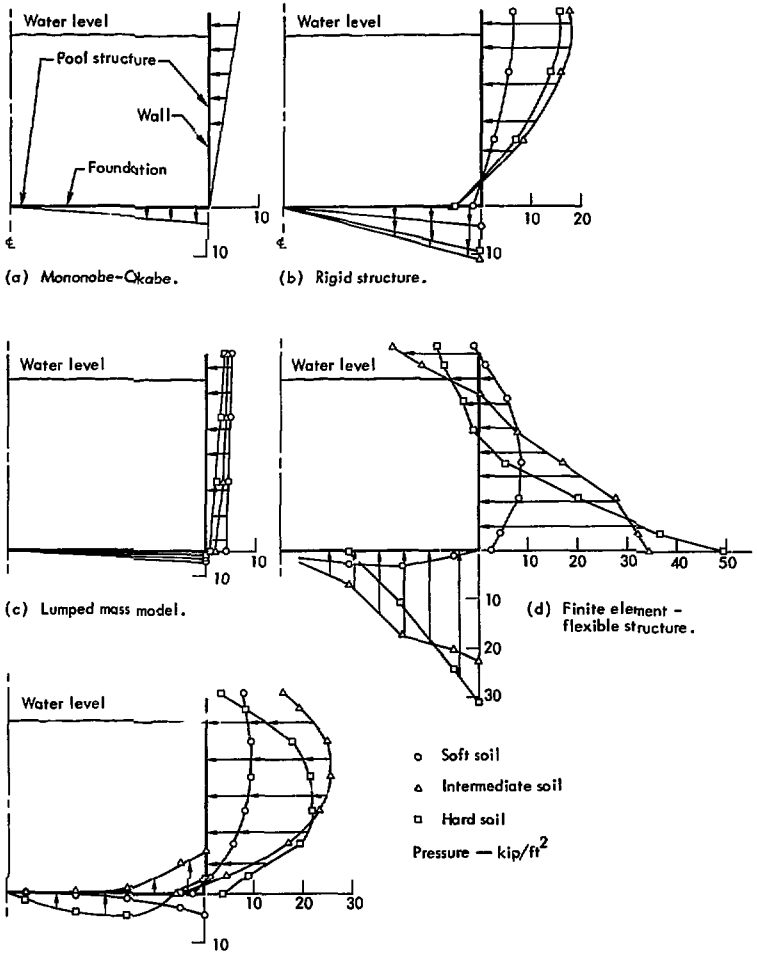

Fig. 59. Results — pressure distributions.

The sidewall soil pressures predicted by the M-O theory and the lumped mass model were in substantial agreement with each other. The former predicted a linear distribution varying from 0 to 6 kip/ft^2. The latter method resulted in pressures between 1 and 5.2 kip/ft^2 for all soil conditions. For the soft soil case, results of the other two methods were also in reasonable agreement with the M-O and lumped mass methods. Peak pressures (for soft soil) predicted by the rigid-structure-with-imposed-displacements method and the finite element method range between 5.6 and 9.5 kip/ft^2.

However, for the intermediate and hard sites, the M-O and lumped mass wall pressures were less than half those predicted by the other two methods. For example, the imposed displacement and finite element methods resulted in peak pressures (for intermediate and hard sites) ranging from 15.6 to 44.0 kip/ft2. The M-O method and the lumped mass model predict lower wall pressures because they do not account for site response characteristics.

The rigid structure model with imposed displacements should be compared with the finite element results for a rigid structure. The comparison is quite favorable. The wall pressure distributions are similar. The peak wall pressures produced by the imposed displacement method are 5.6, 17.4, and 15.6 kip/ft^2 for soft, intermediate, and hard soil, respectively. The finite element (rigid structure) peak pressures are 9.5, 25.0, and 22.0 kip/ft^2. The intermediate site results are largest because the spectral acceleration is largest for that site. Figure 59e indicates that the finite element pressure distribution falls off at the top of the structure, particularly for intermediate and hard sites. By contrast, Fig. 59b indicates that the imposed displacement method produces the peak pressure at this point. Although the imposed displacement method yields wall pressures comparable to those from the finite element method, it overlooks the soil-structure interface shear. These forces are important to the overall design of the structure.

The results of the finite element analysis indicate that site properties have a significant effect on the seismic response of deeply embedded structures. The finite element method provides a way to account for this and yields higher design loads. It also accounts for effects unforeseen by the analyst, such as the fact that soil-structure shear forces, instead of the foundation pressure, counteract the overturning moment. The plane-strain assumption introduces its own problems, however. The analyst must decide what mass and stiffness to use in the pool structure model. We felt the mass was of less importance and thus varied only the stiffness.

MANPOWER AND COMPUTER EFFORT

Table 21 indicates the manpower and computer effort we estimate would be required to conduct each of the analyses. These estimates are intended as indicators of the relative effort required. They assume the analyst is familiar with the method and the structure. Having defined the earthquake loads, the designer would

Table 21. Manpower and computer effort— FRSS pool structure.

Method	Manpower (man-weeks)	Computer time (CDC 7600-min.)
Equivalent static		
M-O theory	0.2	0
Dynamic		
Imposed displacement	0.2	0
Lumped mass	0.5	1
Finite element	1	5

use them to statically design the structure. This procedure would be essentially the same, regardless of the method used to determine the loads. The design effort is not included in Table 21.

CONCLUSIONS

The analysis results indicate that the response spectra-finite element method should be used to determine loads on deeply embedded structures. It alone accounts for all the factors the results show to be important: site response characteristics, soil stiffness, structure stiffness, and soil-structure interface shear forces. In addition this method consistently produces higher loads than the other three methods.

Two additional benefits accrue from the use of the finite element method: (1) the same model (which accounts for much of the manpower required) could be used for the vertical ground motion problem, and (2) the model would also allow the use of strain-compatible soil properties if this became desirable.

The rigid structure model with imposed displacements gave reasonable sidewall pressures with relatively little effort. However, it does not account for soil-structure interface shear and thus does not predict the overall load path correctly. It is possible that this method could be modified to include all the important features of the structure-site response to ground motion. In many cases, however, the analyst would have to know what to expect beforehand in order to use such a method. The finite element method relieves him of that burden without requiring a great deal more effort.

Acknowledgment

The authors wish to acknowledge the assistance and encouragement of V. N. Karpenko, leader; and C. E. Walter, deputy leader; Nuclear Test Engineering Division, Mechanical Engineering Department, Lawrence Livermore Laboratory.

We would like to particularly thank H. Stelling, U.S. N. R. C., Office of Standards Development, for providing guidance and support throughout this study.

We also appreciate the time spent by R. I. Newman and his associates at the Barnwell Nuclear Fuel Plant and E. Gallagher and his associates at Bechtel Company. Their assistance and cooperation have been most helpful.

Appendix A

Existing Fuel Reprocessing Facilities

The information presented in this Appendix was taken from The Safety of Nuclear Power Reactors and Related Facilities.[19] For more detailed information, consult this document.

Nuclear reactor fuel assemblies must be replaced periodically. Each year, typical large (1000 MW) power reactors discharge from 25 to 40 tons of spent fuel, in 60 to 200 fuel assemblies. These spent fuel assemblies are sources of heat and intense radioactivity.

The function of a fuel reprocessing plant is (1) to recover the residual fuel materials (uranium and plutonium) in a pure form suitable for re-use, and (2) to isolate radioactive wastes for storage and ultimate disposal. Commercial fuel reprocessing plants use recovery processes that are variations of the recovery process that has been used in ERDA-operated facilities for many years.

The ERDA plants in Richland, Washington, and Savannah River, South Carolina, have done production-scale reprocessing of irradiated low-enrichment nuclear fuels. The ERDA Chemical Processing Plant at the Idaho National Engineering Laboratory has been operated for the past twenty years to recover high-enriched uranium from irradiated nuclear fuels.

The first commercial reprocessing plant in the U.S. was the Nuclear Fuel Services facility in West Valley, N.Y. It began operation in 1966 with a nominal capacity of 300 metric tons per year of low-enriched uranium fuels irradiated in light-water power reactors. Presently the plant is shut down for modification to increase its reprocessing capacity and to improve its process.

The Midwest Fuel Recovery Plant, owned by General Electric Company in Morris, Illinois, was originally expected to begin operations in 1973 with a nominal capacity of 300 metric tons per year of low-enriched uranium fuels. However, economics and technical problems related to the chemical process have occurred and the plant is not yet operational.

A third commercial plant, the Barnwell Nuclear Fuel Plant, is being constructed in Barnwell County, South Carolina, for Allied-General Nuclear Services and is scheduled to begin operations in 1976 with a nominal fuel reprocessing capacity of 1500 metric tons per year of low-enriched uranium fuels from light-water power reactors. A plant of this capacity is considered typical of future recovery plants.

REPROCESSING TREATMENT

The process treatment steps in a reprocessing plant are illustrated in Fig. A-1. After a normal period of storage at the reactor of about 150 days to allow decay of greater than 95% of the sources of heat and radioactivity, the spent fuel is transported from the reactor to the reprocessing plant in heavy, shielded casks. The casks are designed to hold either seven Pressurized Water Reactor or eighteen Boiling Water Reactor fuel assemblies weighing some 65 tons.

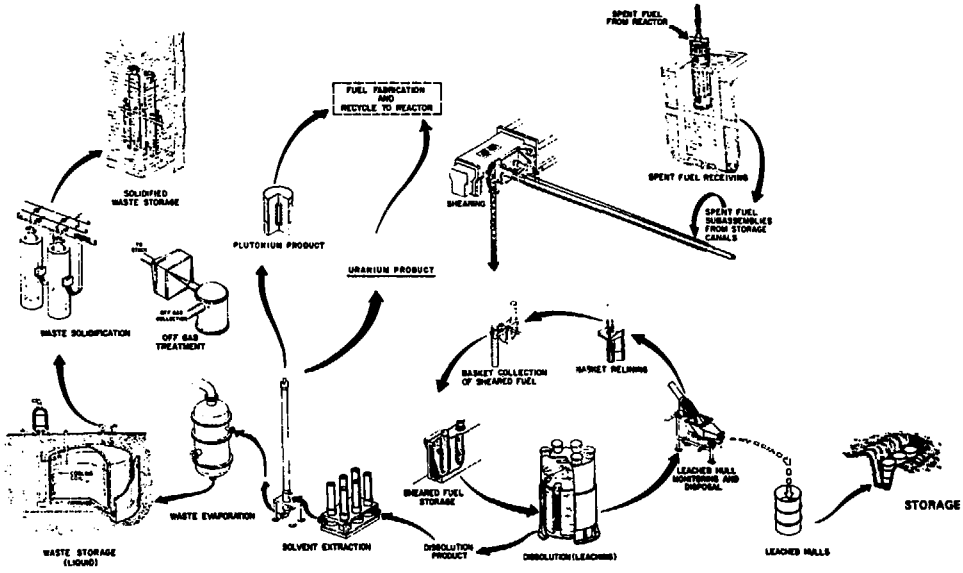

Fig. A-1. Reprocessing of spent power reactor fuel.[19]

The casks are lifted from the transport vehicle (truck, barge or railroad car) by a crane and lowered to the bottom of the cask unloading pool (more than 50 ft below the water level). The water provides shielding from the radiation when the fuel is removed from the cask. All fuel handling and storage operations are conducted below a water depth that is safe for radiation shielding. The fuel elements are transferred to storage canisters and stored in racks located in the adjacent fuel storage pool.

The first step in reprocessing is to shear the long fuel assemblies into approximately 1-in. pieces to expose the fuel material for dissolving in nitric acid. The sheared fuel is placed in the nitric acid, where the fuel material containing the uranium, plutonium, and fission products is dissolved, leaving the cladding hulls as a residue. The dissolved solution containing the uranium, plutonium, and fission products is transferred to the feed tank for the purification process. The hulls are placed in containers and transferred to the solid waste storage area.

Uranium and plutonium usually are recovered and purified by a solvent extraction process. Reprocessing conditions are such that the uranium and plutonium are extracted while the other fission products remain in the liquid waste. The liquid waste is transferred to the waste treatment system, and the uranium and plutonium are separated from each other in a second extraction operation.

The purified uranium and plutonium products are packaged in licensed shipping containers and shipped to the fuel fabrication plant as solid plutonium oxide, solid uranium oxide, or liquid uranium hexafluoride. All the solvent extraction reprocessing plants are considering conversion of the recovered uranium to uranium hexafluoride for direct recycling to a uranium enrichment plant.

TREATMENT OF LIQUID RADIOACTIVE WASTES

The latest reprocessing plants are designed to reduce to a minimum the release of liquid radioactive effluent under normal operating conditions. The highly radioactive wastes from the solvent extraction systems are concentrated by evaporation to decrease the volume to be stored. The vapor from the evaporator typically contains less than one-hundred-thousandth (10^{-5}) of the radioactive material in the original waste, along with acid and water. The acid is separated for re-use and the water vapor may be monitored and discharged up the stack or condensed and recycled. The evaporator concentrate may be sent to either a liquid waste storage tank for interim storage or a feed tank for calcination to a dry solid. Liquid wastes are stored as acidic solutions in stainless steel tanks or as alkaline solutions and slurries in carbon steel tanks.

Liquid-waste storage tanks are in underground stainless steel-lined concrete vaults. Decay heat is removed during storage by use of water-cooling coils submerged in the waste. Federal regulations require the solidification of the wastes within a five-year period after collection, and transfer of the solids to a Federal repository within ten years.

The stainless steel cylinders containing the solidified high-level wastes

are sealed and stored in racks under water in canals prior to shipment to a Federal repository. Circulating water removes the radioactive decay heat from the cylinders.

TREATMENT OF GASEOUS EFFLUENTS

The gaseous effluents, including building ventilation air, are treated to remove to the extent required by regulation chemical and radioactive contaminants before the gases are released. The principal radioactive materials in the untreated off gas are tritium, krypton, iodine, and radioactive particulates suspended in the air. The principal nonradioactive contaminants are nitrogen oxides.

Gas from the spent fuel shearing and dissolution steps and from venting of process vessels contain the highest amounts of radioactive materials. They are given extensive treatment to remove radioactive contaminants and nitrogen oxides prior to discharge through a tall stack. The treatment involves primary and secondary scrubbers, absorbers, and high-efficiency particulate air (HEPA) filters. The air from the process cells and other parts of the building also passes through HEPA filters, or a deep-bed sand filter, before entering the stack.

This type of treatment of gaseous effluent removes at least 99.9% of the iodine from the off gas and essentially all the particulate matter. The krypton and tritium are not removed and are discharged to the atmosphere. Atmospheric dispersal of these radionuclides reduces the off-site concentrations to levels that are well below those considered acceptable in current federal regulations. The need for the removal of krypton and xenon from the stack gases and of tritium from process off gases and methods to do this are currently under examination.

PLANT SAFETY CONSIDERATIONS

Because of basic functional differences between fuel reprocessing plants and nuclear power plants, the structure and safety systems of fuel reprocessing plants differ in some respects from those used in nuclear power reactors. Nevertheless, the same safety philosophy is applied to both. Some of the differences that influence safety systems are:

(1) The fuel reprocessing plant does not have the high temperatures or pressures that are associated with power reactors.

(2) In a power reactor, most of the radioactive materials are encapsulated in the fuel assemblies, but in the fuel reprocessing plant the radioactive materials are released from the fuel and must be handled by the reprocessing system.

(3) A decay time (the time between fuel element discharge from the reactor and the start of reprocessing operations) allows much of the fuel radioactivity, which is in the form of short-lived radionuclides, to disappear.

(4) The reprocessing plants are designed to handle fuel from 10 to 50 large (1000 MW) reactors. Thus the quantity of fuel at a reprocessing facility is much greater than the amount of fuel at a reactor.

Structures and Confinement Barriers

Fuel reprocessing plants are designed with multiple confinement barriers for control of radioactive materials. Postulated accidents involving acts of nature or other external forces are the same as those that are assumed for the design of nuclear power plants. The general policy is that process and confinement systems will be designed, tested, routinely inspected, and maintained so that exposure to credible external events or forces (loss of power, earthquakes, tornados, floods, hurricanes, impaction by moving vehicles, etc.) will not impair the ability to shut down the plant safely and maintain safe shutdown conditions.

The structures, systems, and equipment are classified according to their function and the degree of integrity required for plant safety. In a typical new plant, the classification according to usage might be:

Seismic Category I structures, systems and equipment are those whose failure could cause uncontrolled release of radioactive materials or those whose operation is required to effect and maintain a safe plant shutdown. Systems and equipment in this class are designed, constructed, and inspected to withstand all postulated loadings without loss of function.

Seismic Category II structures and systems are those whose failure would not result in an uncontrolled release of radioactive materials and whose function is not required to effect and maintain a safe plant shutdown.

Ventilation and Off Gas Systems

The process building is supplied with cleaned and conditioned air. The air then flows to limited access zones and finally to restricted access zones. The ventilation air flow is maintained in the desired direction by providing progressively lower pressure levels in zones of increasing radioactive contamination. Air from the process cells is combined with ventilation gases, refiltered, and monitored for activity before discharge through the ventilation fans and plant stack to the environment.

Process Safety Systems

Process safety systems minimize the probability of occurrence of accidental conditions that could potentially disperse radioactive materials and/or mitigate their consequences. These accidental conditions include process upsets, equipment leaks, fire, chemical explosion, or nuclear chain reactions. Such safety systems are carefully designed and constructed and incorporate use of both engineered and administrative controls.

Process operations and enclosures are highly instrumented with sensors for radiation level, temperature, pressure, volume, weight, flow rate, and material concentration. Such instrumentation systems detect process upsets; equipment leaks; and changes in mass, concentration, moderation, or neutron absorber content that could lead to nuclear criticality conditions. Criticality incidents are prevented in a fuel reprocessing plant by assuring that the individual systems are subcritical and that any feasible assembly of systems is subcritical. Plant designs treat hazardous chemicals in conformance with the practice in both nuclear and nonnuclear industries. Emergency electric power generators are provided to

maintain vital services, and emergency sources of cooling water are available in case of failure of tne primary water supply.

The control room of the plant is designed to be a Seismic Category I structure that is isolated from the process by remote instrument systems so that no transfer of radioactive materials into the control room can occur.

Appendix B

Site Response Analysis

INTRODUCTION

In this section, we derive seismic input at the foundation level for Reprocessing Plant Structures with foundations at any level.* There are presently no official NRC quidelines regarding the seismic input for these types of structures. However, we expect that, when written, the quidelines will be based on the same logic as the corresponding guidelines for nuclear power reactors. Therefore, in this analysis, we assume a given surface response spectrum and calculate the resulting response spectra at other soil depths.

This is an important calculation that has more significance than simply providing the seismic input to our structural analyses, for it also provides an evaluation of the response spectrum variation with depth. If the variation is small then it may be sufficient to apply the surface response spectrum as input to embedded foundations and thus avoid a site response calculation. On the other hand, site response calculations are required if our results show that the variation is large.

Because of the absence of appropriate data for a representative variety of sites, we will base our evaluation on calculated results rather than empiricism. We will use the SHAKE code because results from SHAKE compare favorably with the little data available.

*Because we perform free-field calculations, the input will be valid only for structures where there is no soil-structure interaction. We enlarge on this point later.

CALCULATION TECHNIQUES

Typical Sites

Figure B-1 illustrates the three typical sites chosen for analysis. The order of increasing hardness is consistent with average acoustic shear wave velocity. We take the water table to be at bedrock (the base of each deposit) for each site. Bedrock is assumed to be infinitely hard and the lower half of each deposit is a gradation layer between the relatively soft upper soils and the rigid bedrock half space. We include this gradation layer to smooth out rapid changes in soil properties and thus minimize potential numerical difficulties.

We take the density of each layer to be constant, and we assign a different shear stress-strain function to each layer. Soils are exceedingly nonlinear, and therefore we use the shear modulus-shear strain function presented by Seed and Idriss.[6] These curves are shown in Fig. B-2. The shear modulus function for typical rocks and clays is fairly straight-forward; the shear modulus function for sand is more complex because its shear modulus is very sensitive to overburden pressure. The functional dependence on pressure is $p^{1/2}$; therefore the shear modulus of a typical sand at a given overburden pressure is the function in Fig. B-2 times $p^{1/2}$.

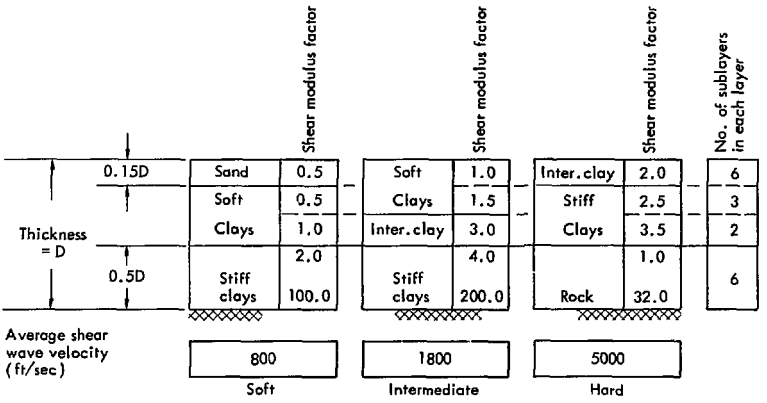

Fig. B-1. The three sites used in the calculations.

To allow for shear modulus functions slightly different than those in Fig. B-2, we introduce a shear modulus factor for each layer. This factor multiplies the appropriate function to define the shear modulus used in that layer. Figure B-1 includes the shear modulus factors that we used for each layer; Table B-1 gives the corresponding low strain (10^{-4}%) acoustic shear modulus for each layer. We find that our calculations were very insensitive to the damping factors used; we therefore used directly the damping factor functions given in Ref. 6 and reproduced in Fig. B-3.

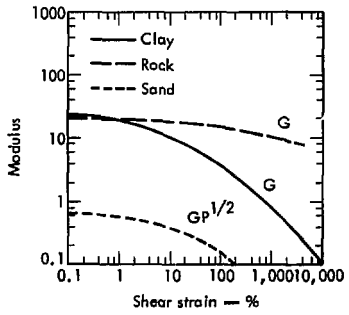

Fig. B-2. Shear moduli used in the calculations.

Soil Thicknesses

In our calculations, we determine the response of each of the soil deposits for total thicknesses of 200 and 400 ft. We include this parameter to assess the sensitivity of the response to a possible uncertainty in the assumed soil depth of a site. These depths represent, in our judgment, typical depths to bedrock in the eastern United States.

Seismic Input to Each Deposit

We shall require that the bedrock motion be such that a specified typical response spectrum be recorded at the surface of each deposit. We feel that the

Table B-1. Soil properties used in the calculation.

Soil type	Unit weight (kip/ft^3)	Range of 10^{-4}% strain shear moduli above gradation layer (kip/ft^2)
Sand	0.085	701 - 2330[a]
Soft clays	0.090	1150 - 3450
Intermediate clays	0.090 - 0.120	4600 - 6900
Hard clays	0.120	5750 - 8050
Soft rock	0.120	(used only in gradation layer)

[a]Including the effect of overburden.

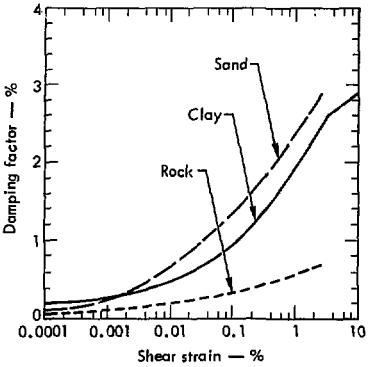

Fig. B-3. Damping factors used in the calculations.

most comprehensive comparison of earthquake response spectra was recently prepared by J. A. Blume and Associates for the USAEC.[5] Their statistical investigation of 33 earthquake records resulted in a statistically-most-probable response spectrum (normalized to 1.0 g) and spectra for plus and minus one standard deviation. We shall take their most probable response spectrum as our surface response spectrum (SRS).

We used the SHAKE code to perform the dynamic response calculation. Because the code calculates the soil response in the frequency domain, we can apply the seismic input anywhere in the deposit and allow the code to calculate the motion elsewhere by means of transfer functions. In our application, it is most convenient to consider the SRS as the seismic input and to use the code to calculate the equivalent bedrock accelerations.

Because SHAKE requires the input to be in the form of an accelerogram, we used the code SIMEAR to derive an equivalent synthetic accelerogram from the SRS. In generating the accelerogram for the application, we required that: (1) the total duration be 30 sec, (2) the duration of strong shaking be 8 sec, and (3) the strong shaking start after 9 sec. Figure 7 shows the calculated accelerogram, normalized to 1.0 g; in Fig. 6 we compare the response spectrum of the accelerogram to the SRS at 5% damping. The agreement is good, and we therefore take the derived acceleration history, appropriately normalized, as the seismic input to SHAKE.

We considered it important in our analysis to examine the effects of

different intensities of shaking. This parameter will capture the effect of an uncertainty in the magnitude of the causative earthquake. We judged that 0.125 g would be a typical peak surface acceleration for potential fuel reprocessing plant sites and that 0.250 g would be an upper limit. We therefore normalized our synthetic seismogram to each of these two peak accelerations. These two accelerograms were taken as seismic input to the soil response calculations.

Analysis

We made over 30 trial calculations with SHAKE to appraise its sensitivity to input parameters. By trial and error we found that optimum mesh size varied from 2.5% of the entire deposit thicknesses near the surface to 10% at the gradation layer (half the thickness of the entire deposit). The results were less sensitive to sublayer thickness in the gradation layer, except at the very base of the soil where sublayer thicknesses less than 10% of the total thickness were required.

We found that almost all the energy in the accelerogram was carried in frequencies less than 10 Hz; we therefore suppress all acceleration amplitudes at frequencies over 10 Hz. We found that the higher frequencies often cause stability problems in the calculation.

In every calculation but one (which we will discuss in detail later), we required that the code iterate until values of the shear modulus and damping factor changed by less than 5% or for 20 iterations, whichever came first. The maximum number of iterations was never required.

After the calculation was completed, in every case we input the calculated bedrock motion to SHAKE and then recalculated to find the corresponding surface motion. The difference between this accelerogram and the surface accelerogram originally input was to provide a check on the original calculation. In every case but one, the differences were negligible.

In summary then, we have selected the three soil deposits as typical fuel reprocessing plant sites. We consider each to have two thicknesses (200 ft or 400 ft), and the dynamic soil properties (shear moduli and damping) of each site are taken to be nonlinear. We calculate the response of a specified surface accelerogram down to bedrock twice for each site, once with a peak acceleration of 0.125 g and again with a peak of 0.250 g. The selection of these parameters (three sites, two thicknesses, and two peak accelerations) gives twelve different response calculations. The results of these calculations are given below.

RESULTS AND DISCUSSION

We first present the results of each calculation and then compare them. Table B-2 briefly summarizes the twelve runs; Figs. B-4 through B-9 give more detailed results. In each case we summarize relevant site properties and give the shear modulus, shear strain, and response spectra variation with depth. All the spectra here, as well as those following, are for 5% damping.

It is important to remember, while examining the results, that we have specified the surface motion and have calculated the motion elsewhere. Thus we will not see fundamental site periods in the response spectrum emerging at the

Table B-2. Summary of results for the 12 runs.

Run ID	Site hardness	Site thickness (ft)	Peak surface acceleration (g)	Calculated peak bedrock acceleration (g)	Number of iterations to 5% accuracy
1	Hard	200	0.125	0.08	4
2	Hard	200	0.250	0.157	4
3	Hard	400	0.125	0.070	4
4	Hard	400	0.250	0.219	4
5	Intermediate	200	0.125	0.06	4
6	Intermediate	200	0.250	0.115	5
7	Intermediate	400	0.125	0.058	4
8	Intermediate	400	0.250	0.32	6
9	Soft	200	0.125	0.065	5
10	Soft	200	0.250	0.28	8
11	Soft	400	0.125	1.32	15
12	Soft	400	0.250	(——)	(——)

surface; the peak and its period (0.166 sec) have been fixed (see Fig. 6).

The general trend of the results is that as the sites become softer, the depth variation of the secondary peaks in the response spectrum increases while the primary peak varies in a much more complex way, generally displaying a decreased variation. Furthermore, the spectral accelerations at depth significantly exceed the accelerations of the surface on only the softest sites. This is very important, for its shows that for all but soft sites, it is conservative to apply the surface response spectrum to foundation levels below grade. We shall illustrate these trends in the following discussions.

Hard Sites (Figs. B-4 and B-5)

Note the consistency of shape of the response spectrum in Figs. B-4 and B-5. There appear to be no drastic frequency shifts of spectral peaks; rather we observe a simple acceleration amplitude scaling at each frequency. Indeed, we would expect that nonlinear processes like large frequency shifts would be least in the hardest sites. Another important observation is that the surface response spectrum generally bounds all other response spectra. Further, for increasing softness, we see a decrease in variations in the spectral peak and an increase in variations in the secondary peak. Note that for the hardest sites (Fig. B-4) the variation in spectral peaks from the surface to 25-ft depth is very large; the spectral peaks between these two levels vary by a factor of 2. The minor exceptions to these generalizations are probably explained by our inability to order the sites correctly by hardness.

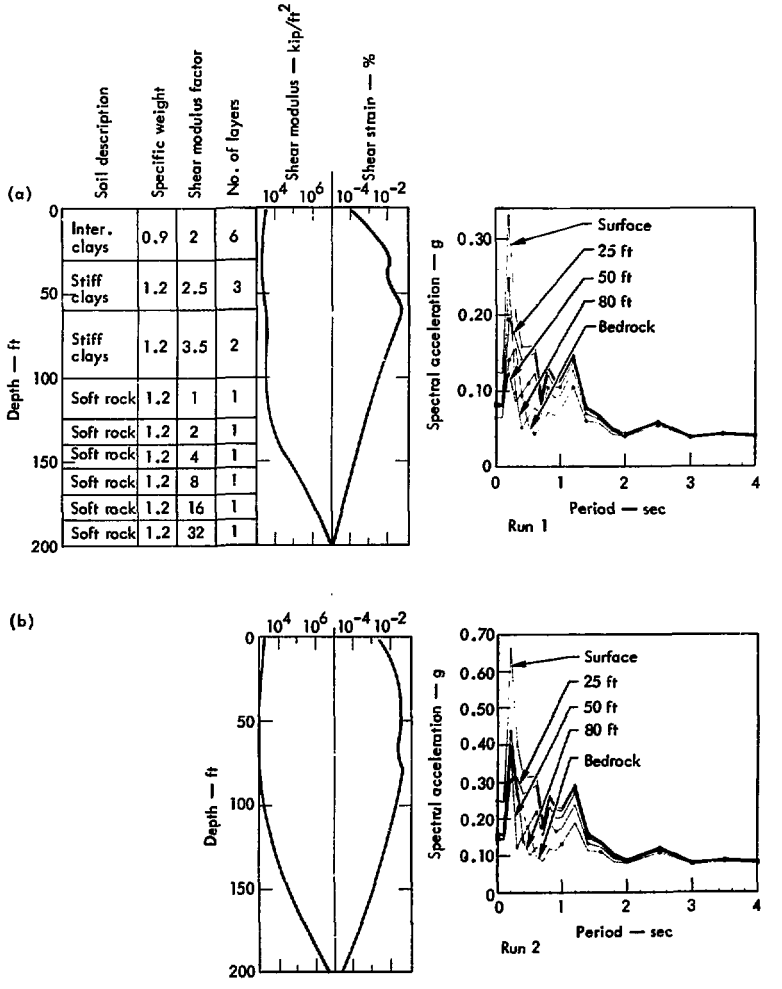

Fig. B-4. Results hard site, 200 ft depth.

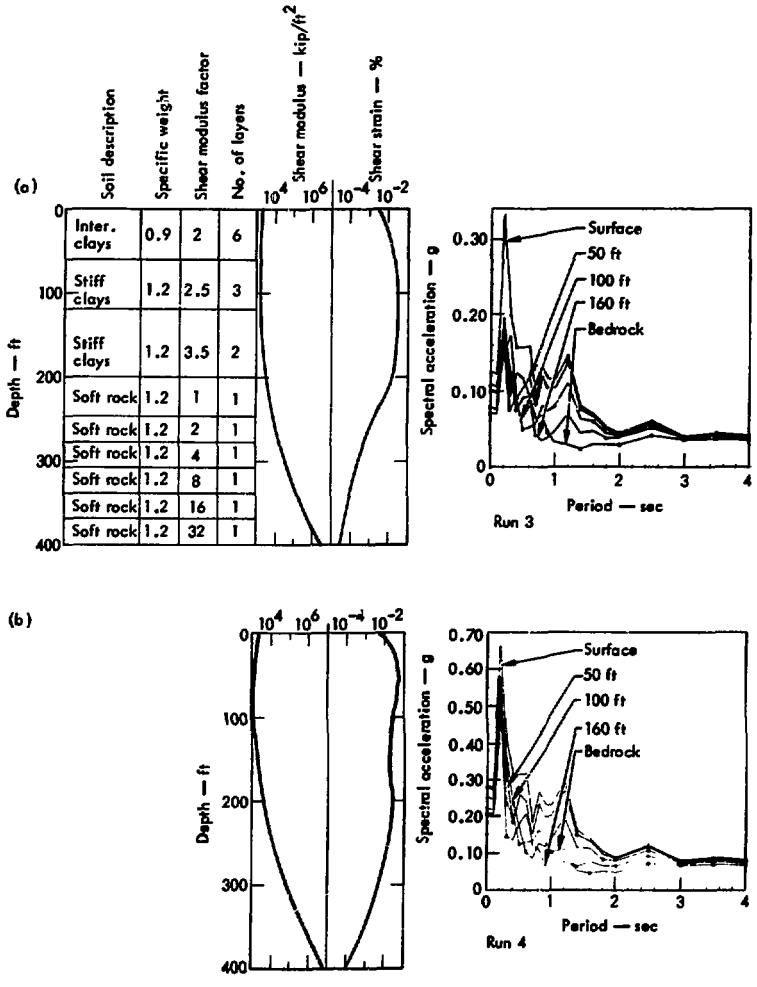

Fig. B-5. Results hard site, 400 ft depth.

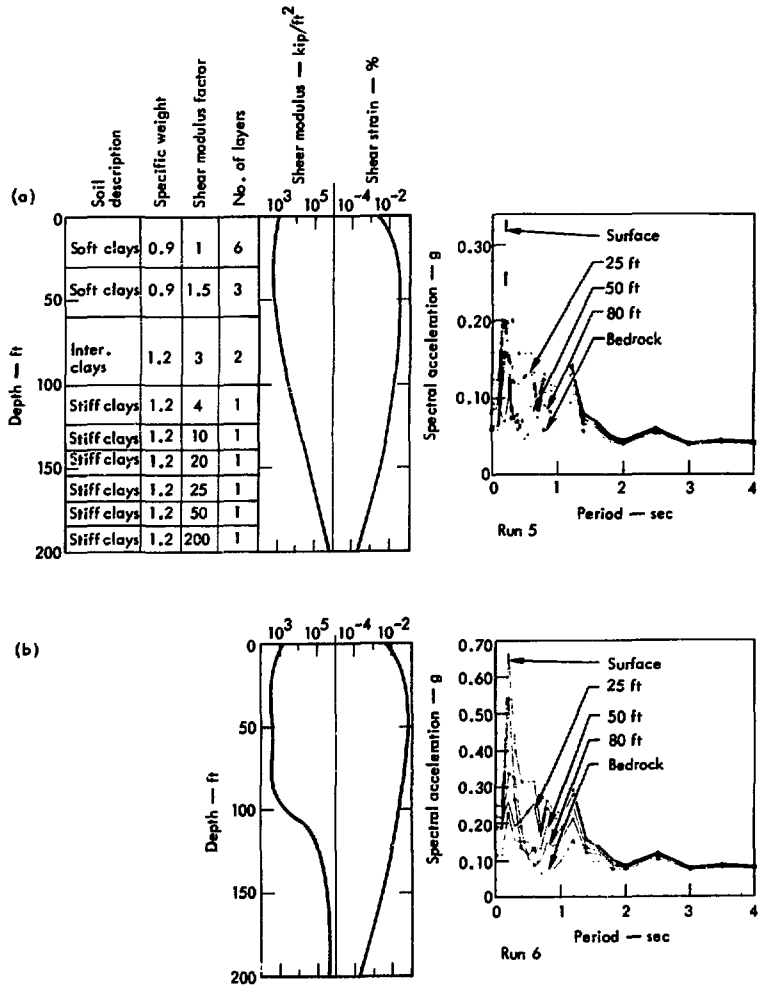

Fig. B-6. Results intermediate site, 200 ft depth.

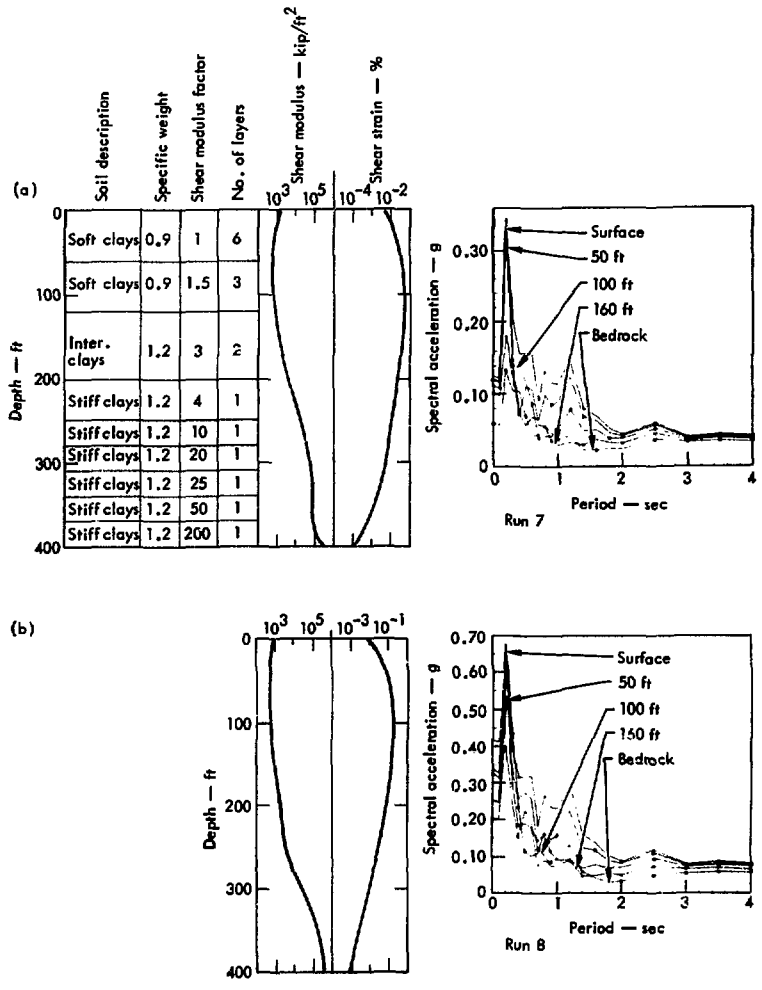

Fig. B-7. Results from intermediate site, 400 ft depth.

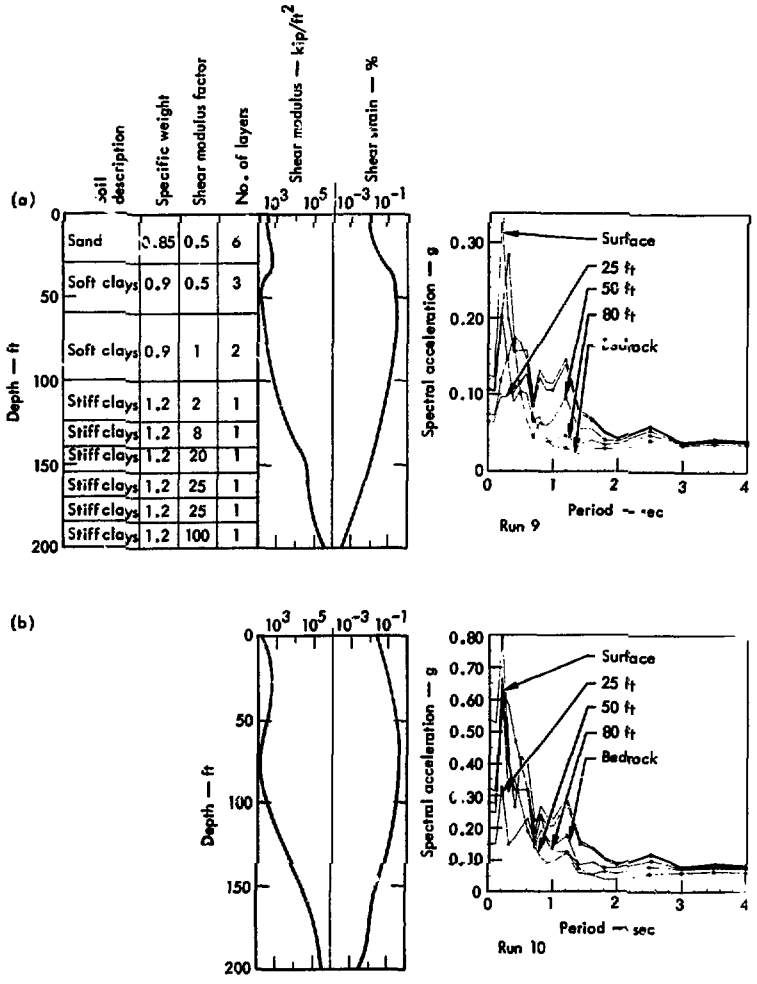

Fig. B-8. Results from soft site, 200 ft depth.

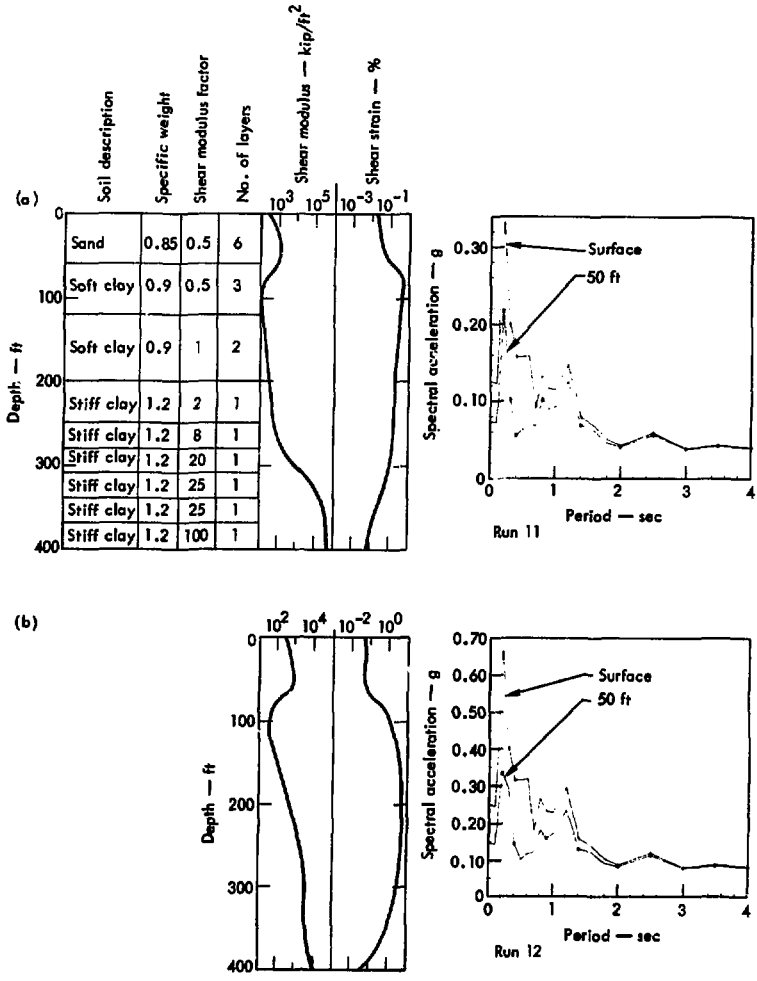

Fig. B-9. Results from soft site, 400 ft depth.

Intermediate Sites (Figs. B-6 and B-7)

We see here a continuation of the trends started with the hard sites: decreasing variation of the primary peaks and increasing variation of the secondary peaks with the surface response spectrum being a bounding spectrum. In Fig. B-6 we see the beginning of appreciable variations in the secondary peaks along with a negligible variation in the primary peaks. Nonlinear effects are still not manifested in large frequency shifts, even through Run 8 (Fig. B-7).

Soft Sites (Figs. B-8 and B-9)

Our results become both more interesting and more complex with the soft sites. First, we begin to observe some frequency shifting of spectral peaks. Second, it can no longer be said that the surface spectral accelerations exceed all others; we see them being exceeded in Fig. B-8a between 0.25 and 0.6 sec and in Fig. B-8b between 0.0 sec and 0.8 sec. We believe these to be genuine results and not the result of the numerical instabilities that plagued the remaining two runs.

The last two runs (Figs. B-9a B-9b) had some numerical difficulties that we believe resulted from the fact that these thick, soft sites cannot support the level of bedrock shaking required for a 0.125-g or 0.250-g surface acceleration. No matter how hard we made the gradation layer the shear modulus in the layers close to bedrock would tend to zero and the strains and accelerations would approach infinity. While Run 11 terminated normally, it took 15 iterations, and the gradation layer was becoming increasingly soft. Run 12 terminated due to an instability after five iterations; we re-ran it to four iterations to get the results in Fig. B-9b. We did this because we observed that SHAKE converged very rapidly to zero error strains and stresses in the uppermost layers, and that these results might have meaning even if results from greater depths might not. Accordingly, in Fig. B-9a and b we overlay plots of the spectra from the surface and from 12.5% of the deposit depth.

EFFECT OF VARIATIONS IN SITE HARDNESS, PEAK SURFACE ACCELERATION, AND SITE THICKNESS

We now turn to comparison of the results. We first compare the hard, intermediate, and soft sites for a given thickness and surface g-level. We then compare the response of each site for the different g-levels. Finally, we examine the effect of site thickness by comparing responses of the same site for both thicknesses, at a given g-level.

Effect of Site Hardness

Figure B-10 compares the response of sites of different hardness of the same level of surface shaking and the same deposit thickness for spectra at the 12.5% total depth level. The results are very complex and it is difficult to generalize from them. However, one thing is clear: the longer-period spectral accelerations are least affected by site hardness, while those accelerations near the fundamental period of the site (0.10 - 0.50 sec) are greatly affected. We might therefore expect that the transfer function for all these sites is highly peaked around the fundamental period. This apparent

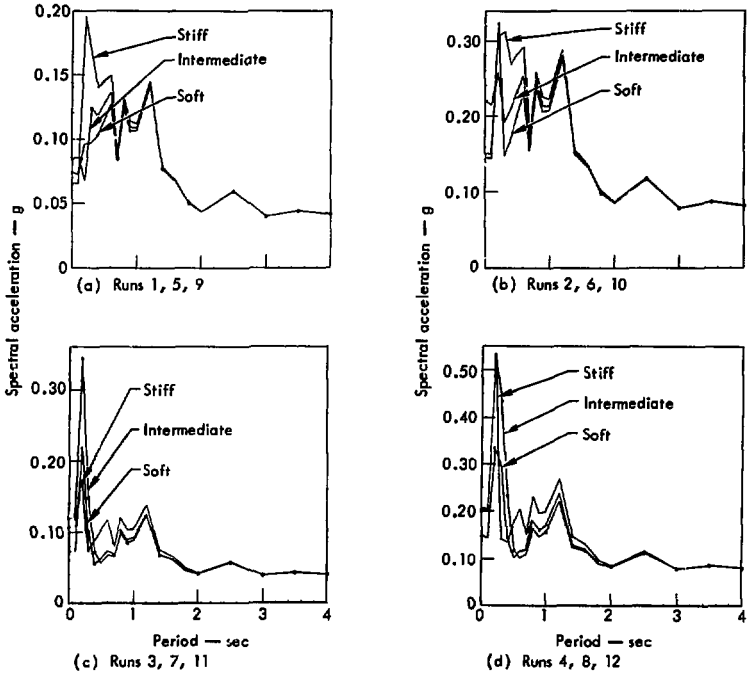

Fig. B-10. Comparisons between different site hardnesses.

complexity is due to the difficulty to classify sites by hardness.

Effect of Peak Surface Acceleration

Here we want to consider the consequences of an uncertainty in the peak surface acceleration. To assess this, we normalized the response of each site of a given hardness and thickness to the peak surface acceleration. For example, the spectral accelerations of each layer from Run 1 were divided by 0.125 g and those from Run 2 were divided by 0.250 g, and the resulting spectra were compared at each layer. We hoped that this comparison would quantify the effect of increasing softness with increasing intensity of shaking. Figure B-11 gives this comparison for the 12.5% total depth level.

The comparison for the hardest site (Fig. B-11a) displays exactly what we expect, i.e., the lower intensity gives proportionately higher spectral accelerations at all periods because of less

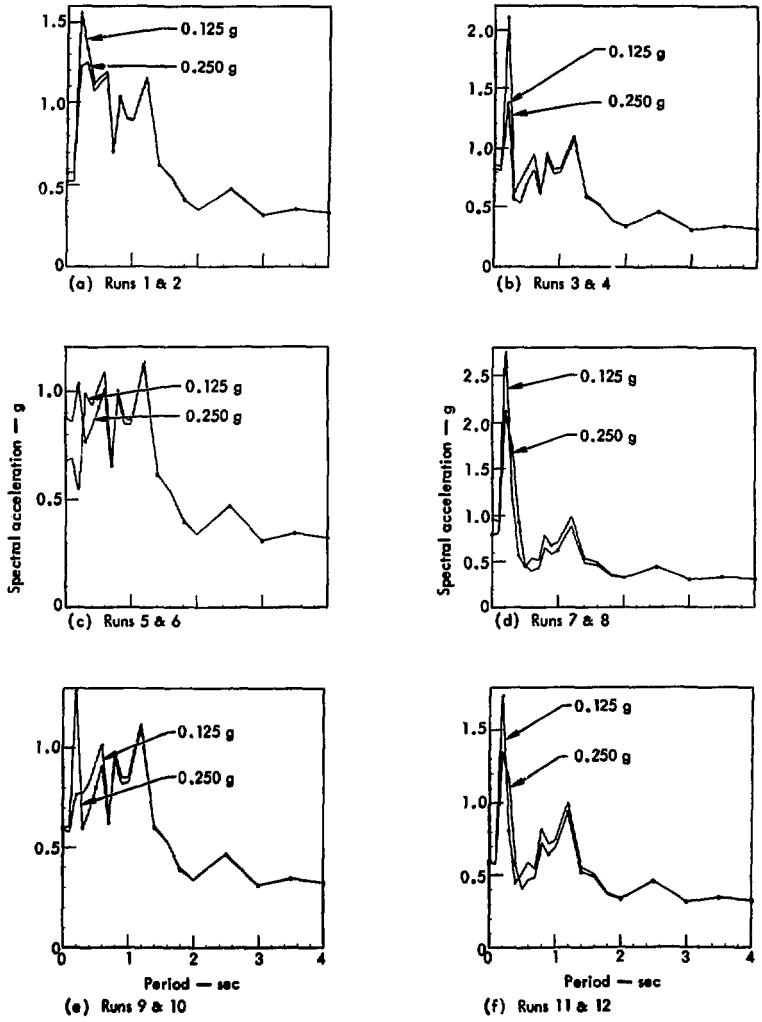

Fig. B-11. Comparisons for different levels of shaking.

dynamic softening.* It is interesting that for all the remaining comparisons in Fig. B-11, the more intense shaking produces proportionately higher spectral accelerations over a small frequency window. This clearly must be the effect of peaks in the site transfer function; it demonstrates that our intuition regarding dynamic softening can sometimes fail us.

In summary, an uncertainty in the estimate of peak surface acceleration can lead to large uncertainties in spectral accelerations at lower levels. These uncertainties can be quantified only by a calculation. However, our calculations show that it is conservative to use the surface response spectrum as the response spectrum for a lower level.

Effect of Site Thickness

In this section, we consider the effect of an uncertainty in the site thickness. Figure B-12 compares the spectra of the 12.5% total depth level for sites of a given hardness and given peak surface acceleration. For example, in Fig. B-12a we compare spectra for Run 1 and Run 3. Here we see that the peak spectral acceleration for the 200-ft-thick site just slightly exceeds that for the 400-ft site. For increasingly softer sites, the spectral peaks for the 400-ft sites exceed those of the 200-ft sites, the greatest excess being for the intermediate sites. However, the spectral accelerations of the 200-ft site always exceed those of the 400-ft site at longer periods.

*Site hardnesses depend on the magnitude of shaking. An intense excitation rich in frequencies near the fundamental site period will so violently shake the deposit that it may respond more like a soft site.

These results show that, as in the prior comparison, we must perform a calculation for a proper understanding of the variation.

MANPOWER AND COMPUTER EFFORT

We assume that SHAKE, or a similar code, is compatible with the user's system. SHAKE is user-oriented, and input is exceedingly manageable. A user supplied with the appropriate site information (seismography, hydrology, physical properties of each layer, and a bedrock or surface accelerogram or response spectrum) might spend two man-days acquainting himself with the code and its sensitivity to input by making several trial runs. These might include varying (1) layer and sublayer thicknesses, (2) frequency cut-off for the input accelerogram, (3) materials characteristics of the bedrock half space, (4) length of "quiet zone" that should be added to the accelerogram, and (5) shear-stress relations. The analyst then forms his best soil deposit model and makes his final SHAKE calculations. If there are any uncertainties, he should include them as parameters. This effort, allowing for additional parametric runs, should require two to three man-days. The total effort should, therefore, require less than one man-week.

The computer time required for each of our calculations averages 20 sec on our CDC 7600 computer with 15 sec being CPU time and 5 sec being I/O time. We estimate that a first-time user might require six runs or roughly 2 min of CDC 7600 time to obtain final answers. We judge that the total effort would

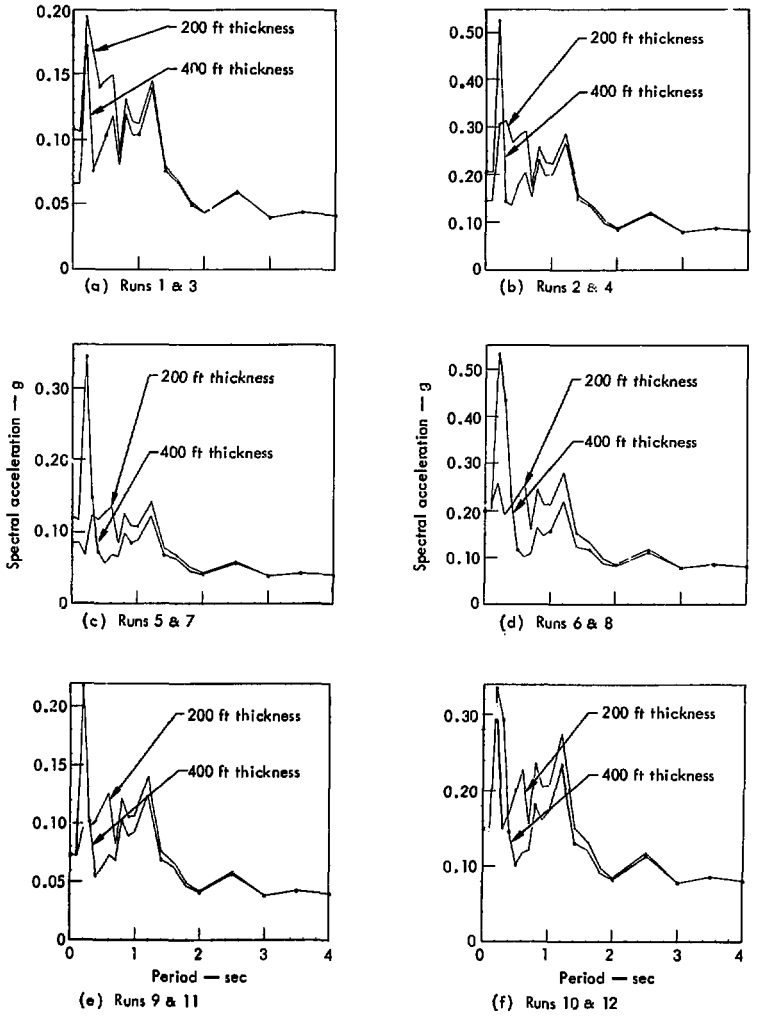

Fig. B-12. Comparisons for different site thicknesses.

require the expense of one man-week and 9 min of CDC 7600 time.

SUMMARY AND CONCLUSIONS

We have selected three different fuel reprocessing plant sites: hard, intermediate, and soft. We have applied a horizontal excitation to each site at bedrock with an accelerogram such that a specified response spectrum is observed at the surface. We shake each site with two levels of shaking and we consider each site to have two different thicknesses. This provides us with 12 calculations, between which we have made extensive comparisons.

Based on the results of these calculations, we conclude:

1. The specified surface acceleration response spectrum is an upper bound for the response spectra at depths below the surface for every site we considered, except for the two softest (Runs 11 and 12).
2. For the range of sites we considered, the effects of site hardness, thickness, and surface acceleration are not easily quantified, probably because of our inability to classify sites by hardness.
3. These results can be used to define the foundation-level seismic input to structures where there is no soil-structure interaction. Where soil-structure interaction is a problem, a separate calculation of the response of the soil-structure system must be preferred. These results provide the input to this calculation.
4. The costs associated with a site response analysis are small.

We emphasize that our results apply only to free-field motion. The input to structures may be very different if there is any soil-structure interaction.

References

1. U. S. Atomic Energy Commission Regulatory Guide 1.60, Design Response Spectra for Seismic Design of Nuclear Power Plants and U. S. Atomic Energy Commission Regulatory Guide 1.61, Damping Values for Seismic Design of Nuclear Power Plants (U. S. Government Printing Office, Washington, D. C., 1973).
2. Document A: Structural Design Criteria for Category I Structures Other Than Containment, Structural Engineering Branch, Directorate of Licensing, U. S. Nuclear Regulatory Commission, Washington, D. C., Internal document, Rev. 1 (June 1974).
3. Final Safety Analysis Report - Barnwell Nuclear Fuel Plant Separations Facilities, Allied-Gulf Chemical Nuclear Services, USAEC Docket No. 50-332 (1973).
4. Generation of Simulated Earthquake (SIMEAR NISEE program brochure, Berkeley, California, December 1972).
5. Recommendations for Shape of Earthquake Response Spectra, U. S. Atomic Energy Commission, Washington, D. C., Rept. WASH-1254 (1973).
6. H. B. Seed and I. M. Idriss, Soil Moduli and Damping Factors for Dynamic Response Analyses, Earthquake Engineering Research Center, University of California, Berkeley, California, Rept. EERC 70-10 (1970).
7. I. M. Idriss, H. Dezfulian, and H. B. Seed, Computer Programs for Evaluating the Seismic Response of Soil Deposits with Non-Linear Characteristics Using Equivalent Linear Procedures, Earthquake Engineering Research Center, University of California, Berkeley, California (1967).
8. P. B. Schnabel, J. Lysmer, and H. B. Seed, SHAKE, A Computer Program for Earthquake Analysis of Horizontally Layered Sites, Earthquake Engineering Research Center, University of California, Berkeley, California, Rept. EERC 72-12 (1972).
9. J. Lysmer, T. Udatea, H. B. Seed, and R. Hwang, LUSH, A Computer Program for Complex Response Analysis of Soil-Structure Systems, Earthquake Engineering Research Center, University of California, Berkeley, California, Rept. EERC 74-4 (1974).
10. J. Isenberg and S. A. Adham, ASCE Power Division 98 (PO2), 279 (1972).
11. R. V. Whitman and F. B. Richart, Jr., J. Soil Mech. Found Div., ASCE 93 (SM6), 169 (1967).
12. 1973 Uniform Building Code (International Conference of Building Officials, Whittier, California, 1973)
13. U. S. Atomic Energy Commission Regulatory Guide 1.92, Combination of Modes and Spatial Components in Seismic Response Analysis (U. S. Government Printing Office, Washington, D. C., December 1974).
14. K. J. Bathe, E. L. Wilson, and F. E. Peterson, SAPIV Structural Analysis Program for Static and Dynamic Response of Linear Systems, Earthquake

Engineering Research Center, University of California, Berkeley, California, Rept. EERC 73-11 (1973).

15. S. Ghosh and E. Wilson, Dynamic Stress Analysis of Axisymmetric Structures Under Arbitrary Loading, Earthquake Engineering Research Center, University of California, Berkeley, California, Rept. EERC 69-10 (1969).
16. W. Flügge, Stresses in Shells (Springer-Verlag, Berlin/Heidelberg/New York Publishers) Third Printing (1968).
17. S. Timoshenko and S. Woinowsky-Krieger, Theory of Plates and Shells (McGraw-Hill Book Company, Inc., New York, 1959).
18. H. B. Seed and R. V. Whitman, "Design of Earth-retaining Structures for Dynamic Loads," presented at short course on Earthquake Resistant Design of Engineering Structures, Berkeley, California, June 1972.
19. The Safety of Nuclear Power Reactors and Related Facilities, U.S. Atomic Energy Commission, Washington, D.C., Rept. WASH-1250 (1973).

MBB/lc/la